Various Structural Design Modifications : para-Substituted Diphenylphosphinopyridine Bridged Cu(I) Complexes in Organic Light-Emitting Diodes

Busch, Jasmin M.

American Chemical Society
2021-02-15

Busch, J M, Koshelev, D S, Vashchenko, A A, Fuhr, O, Nieger, M, Utochnikova, V V & Bräse, S 2021, 'Various Structural Design Modifications : para-Substituted Diphenylphosphinopyridine Bridged Cu(I) Complexes in Organic Light-Emitting Diodes', Inorganic Chemistry, vol. 60, no. 4, pp. 2315-2332. https://doi.org/10.1021/acs.inorgchem.0c03187

http://hdl.handle.net/10138/340238
10.1021/acs.inorgchem.0c03187

unspecified
acceptedVersion

Various Structural Design Modifications: *para*-Substituted Diphenylphosphinopyridine Bridged Cu(I) Complexes in Organic Light-Emitting Diodes

Jasmin M. Busch, [a] Daniil S. Koshelev, [b] Andrey A. Vashchenko, [c] Olaf Fuhr, [d] Martin Nieger, [e] Valentina V. Utochnikova*[f] and Stefan Bräse*[a, g].

[a]Institute of Organic Chemistry (IOC), Karlsruhe Institute of Technology (KIT), Karlsruhe, Fritz-Haber-Weg 6, 76131 Karlsruhe, Germany. E-mail: braese@kit.edu

[b]Faculty of Materials Science, M.V. Lomonosov Moscow State University, 1/73 Leninskye Gory, Moscow, 119991, Russia. E-mail: valentina.utochnikova@gmail.com

[c]P.N. Lebedev Physical Institute, Leninsky Prosp. 53, Moscow, 119992, Russia. E mail: andrewx@mail.ru.

[d]Institute of Nanotechnology (INT) and Karlsruhe Nano-Micro Facility (KNMF), Karlsruhe Institute of Technology (KIT), Hermann-von-Helmholtz-Platz 1, 76344 Eggenstein-Leopoldshafen, Germany. E-mail: olaf.fuhr@kit.edu

[e]Department of Chemistry, University of Helsinki, P.O.Box 55 (A.I. Virtasen aukio 1), 00014 University of Helsinki, Finland. E-mail: martin.nieger@helsinki.fi

[f]M.V. Lomonosov Moscow State University, 1/3 Leninskye Gory, Moscow, 119991, Russia. E-mail: valentina.utochnikova@gmail.com

[g]Institute of Biological and Chemical Systems – Functional Molecular Systems, IBCS-FMS, Karlsruhe Institute of Technology (KIT), Hermann-von-Helmholtz-Platz 1, 76344 Eggenstein-Leopoldshafen, Germany.

KEYWORDS Cu(I) Complexes, 2-(Diphenylphosphino)pyridine derivatives, thermally activated delayed fluorescence (TADF), organic light-emitting diodes (OLEDs).

ABSTRACT: The well-known system of dinuclear Cu(I) complexes bridged by 2-(diphenylphosphino)pyridine (PyrPhos) derivatives $Cu_2X_2L_3$ and $Cu_2X_2LP_2$ (L = bridging ligand, P = ancillary ligand) goes along with endless variation options for tunability. In this work, the influence of substituents and modifications on the phosphine moiety of the NP-bridging ligand was investigated. In previous studies the location of the lowest unoccupied molecular orbital (LUMO) of the copper complexes of the PyrPhos family was found to be located on the NP-bridging ligand and enabled color tuning in the whole visible spectrum. A multitude of dinuclear Cu(I) complexes based on the triple methylated 2-(bis(4-methylphenyl)phosphino)-4-methylpyridine (**Cu-1b-H**, **Cu-1b-MeO** and **Cu-1b-F**) up to complexes bearing 2-(bis(4-fluorophenyl)phosphino)-pyridine (**Cu-6a-H**) with electron withdrawing fluorine atoms over many other variations on the NP-bridging ligands were synthesized. Almost all copper complexes were confirmed *via* single crystal X-ray diffraction analysis. Besides theoretical (TD)DFT-studies of the electronic properties and photophysical measurements the majority of the phosphino-modified Cu(I) complexes was tested in solution-processed organic light-emitting diodes (OLEDs) with different heterostructure variations. The best results of the OLED devices were obtained with copper emitter **Cu-1b-H** in a stack architecture of ITO / PEDOT-PSS (50 nm) / poly-TPD (15 nm) / 20 wt% Cu(I) emitter:CBP:TcTA(7:3) (45 nm) / TPBi (30 nm) / LiF(1 nm)/Al (>100 nm) with a high brightness of 5900 Cd/m² and a good current efficiency of 3.79 Cd/A.

INTRODUCTION

The structural diversity of luminescent Cu(I) complexes is enormous. Many examples were already presented in literature, ranging from polynuclear copper clusters,[1-3] over tetranuclear[4-11] and some trinuclear[12-17] structures to a variety of dinuclear[8, 18-28] and mononuclear[29-37] complexes. Multinuclear copper complexes are of special interest due to luminescence enhancing cooperative effects in case the copper centers are in close proximity. This can be realized by choosing the right chelating ligands, giving also rigidity to the system, which is as well important for a bright emission. For this purpose the famous bidentate 2-(diphenylphosphino)pyridine (PyrPhos) and its derivatives proved to be suitable candidates[18-20, 26, 38, 39], amongst other chelating ligands.[24, 35, 40] With NP-bridging ligands mostly dinuclear Cu(I) complexes of the type $Cu_2X_2L_3$[8, 18, 26] and $Cu_2X_2LP_2$[19, 20] as well as a few of the composition $C_2X_2L_2$[41, 42] (X = I, Br, Cl and L = various PyrPhos derivatives, P = monodentate phosphines) were described in literature. Systems in which especially the iodide based Cu(I) complexes, possess high efficiency thermally activated delayed fluorescence (TADF[43, 44]) and high stability, what makes these complexes promising emitter material candidates for organic light-emitting diodes (OLEDs).[19, 20, 39, 45, 46] *Via* TADF not only the 25% of excitons populating the singlet state (S_1) according to spin statistics can be harvested, also the 75% of triplet excitons (T_1 state) get accessible for light emission with an emission pathway over the singlet state.[40, 47-50] Next to the heavy atom effect allowing phosphorescence and the excitation of lanthanide(III) in coordination compounds,[51-55] this a very promising approach to use the remaining 75% of excitons of triplet nature. Enabling of internal quantum efficiencies (IQEs) of up to 100% and short excited state lifetimes (µs – ms), makes TADF emission favored over the traditional fluorescence[56] and phosphorescence,[57-61] respectively. It would be beneficial to transfer this efficiency of TADF emitters to OLED applications to lower the energy consumption of the devices and facilitate even higher resolutions.[62] Up to date the best OLED characteristics were obtained by vapor-deposited emitting layers based on TADF luminophores.[39, 46, 63-65] However, for large-size OLED panels, including screens for entertainment and lighting technology, the vapor-deposition technique becomes impractical, so scalable and cost effective solution based deposition methods entering the production focus.[64] For these reasons novel solution-processable TADF emitters are worth studying.

The main aim of this work was to study the effect of the groups around the phosphorus atom of the PyrPhos bridging ligand in the class of $Cu_2I_2LP_2$ and $Cu_2I_2L_3$ dinuclear Cu(I) complexes on their photophysical properties and to investigate the performance of these complexes in solution-processed OLED devices with different heterostructures. The basic structure and the different variations of the dinuclear Cu(I) complexes investigated in this study are shown in **Figure 1.**

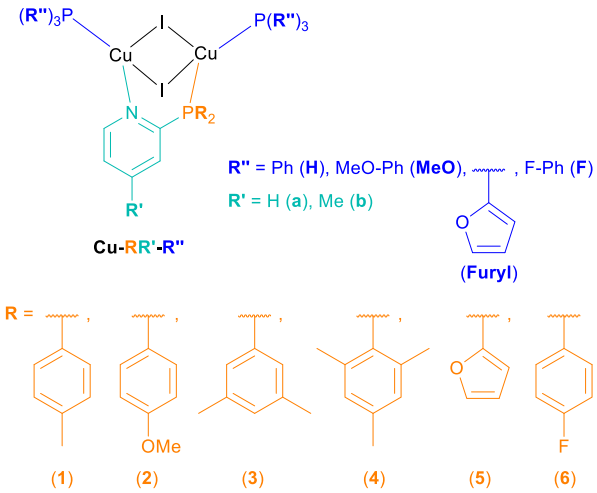

Figure 1. Classification of the dinuclear Cu(I) complexes in this work.

The substituents on the phenyl rings attached to the phosphorus atom of the bridging ligand range from electron donating groups as methyl and methoxy, *via* 2-furyl groups to fluorine atoms as electron withdrawing substituents. As ancillary ligands, triphenylphosphine[19, 20] for possible cross-comparisons and tris(4-methoxyphenyl)phosphine,[20] tris(2-furyl)phosphine[20] and tris(4-fluorophenyl)phosphine[66] were selected for solubility-mediation.

RESULTS AND DISCUSSION

Synthesis of the NP-ligands and Cu(I) complexes

A variety of substituted 2-(diphenylphosphino)pyridine ligands with different phosphine moieties was synthesized to serve as NP-bridging ligands for dinuclear copper complexes of the type $Cu_2I_2L_3$ and $Cu_2I_2LP_2$ (L = NP-bridging ligand; P = ancillary ligand). The phenyl rings of the bridging ligand were modified with additional methyl groups (ligands with the numbers **1**, **3** and **4**, compare **Figure 1**), methoxy groups (ligands with the number **2**) and fluorine atoms (ligand **6a**). In two cases, the phenyl rings were exchanged by 2-furyl (ligands with the number **5**). The additional acronyms **a** and **b** specify the substituent in *para*-position of the pyridine moiety of the NP-ligands (R' = H (**a**), Me (**b**); compare **Figure 1**).

The bridging ligands were obtained by nucleophilic aromatic substitution reactions of the chlorinated pyridine precursors with the corresponding, *insitu* generated, lithiumphosphide species according to the literature protocol with chlorodiphenylphosphine[18] (reaction A, **Scheme 1**) or Pd-catalysed in the presence of NaOAc (reaction B, **Scheme 1**) according to a procedure by Chen and coworkers.[7]

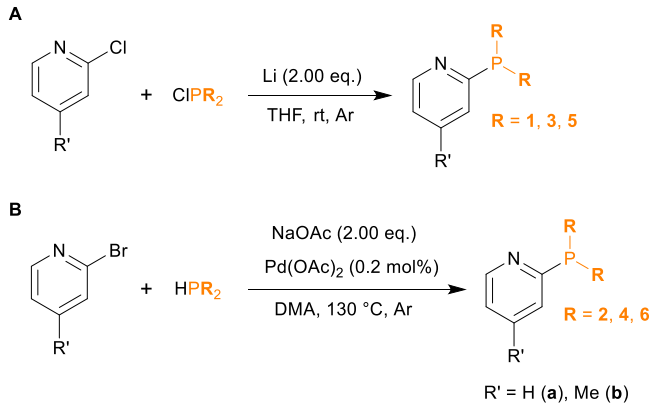

Scheme 1. Two synthesis routes for the NP-ligands, modified on the phosphine moiety.

These phosphino-modified NP-bridging ligands were used in a 1:2:2 ratio with copper iodide and the ancillary phosphine derivative to synthesize the dinuclear complexes in dichloromethane at ambient temperature (**Scheme 2**).[19, 20]

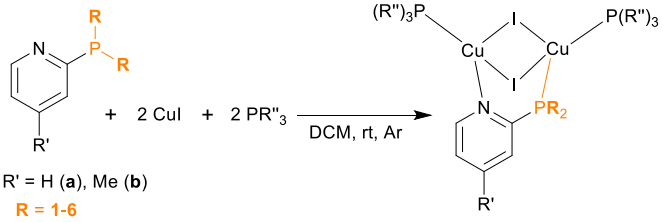

Scheme 2. Copper complex synthesis from copper iodide and the corresponding phosphines according to the stoichiometric ratio in the target complex. For R" compare **Figure 1**.

The Cu(I) complexes with the phosphino-modified NP-bridging ligands were obtained as pale yellow powders in good to very good yields, up to 99%. Not all Cu(I) complexes with the synthesized NP-bridging ligands in this work were accessible. The mesityl groups in ligand **4a** and ligand **4b** are too sterical demanding to form the intended $Cu_2I_2LP_2$ complexes with these ligands. For this reason the bridging ligands **4a** and **4b** did not coordinate to the copper iodide in the reaction. Instead, none luminescent tetranuclear complexes with the used ancillary phosphine ligands (P), $Cu_4I_4P_4$, were formed. Crystals of the $Cu_4I_4P_4$ complexes confirmed the different reaction pathway in these cases. The $Cu_4I_4P_4$ complexes are already described in literature.[67] With all the other bidentate phosphinopyridine derivatives a multitude of different novel Cu(I) complexes was obtained and characterized.

Molecular structures

Almost all molecular structures of the dinuclear Cu(I) complexes could be confirmed by single crystal X-ray diffraction analyses. This enabled a detailed structural study of the copper complexes with the phosphino-modified NP-bridging ligands and set the basis for supporting computational computations for a better understanding of the structures and properties. Hydrogen atoms as well as solvent molecules (if existing) were omitted in all the figures of the Cu(I) complexes for clarity. The bridging ligands were obtained as oils in most cases, due to the enhanced bulkiness resulting of the additional substituents on the phosphine moiety. However, two of the NP-bridging ligands **2b** and **6a** formed microcrystalline parts and molecular structures of the single crystals could be measured and analyzed (see ESI, **Figures S57** to **S60**).

Excluding the ligands **4a** and **4b** bearing mesityl groups on the phosphorus atom, this novel class of complexes tolerates all kind of different substituents from methyl groups (**Figure 2**, **Figure 3**, ESI **Figures S61** to **S65** and **Figures S67** to **S69**) and methoxy groups (**Figure 4** and ESI **Figure S66**) to 2-furyl groups on the phosphorus atom itself of the NP-bridging ligand (**Cu-5a-H**, **Cu-5b-H** and **Cu-5a-F**, compare **Figure 5** and ESI **Figure S71** and **Figure S72**) and fluorine atoms on the PPh_2 group (**Figure 6** and ESI **Figure S73**).

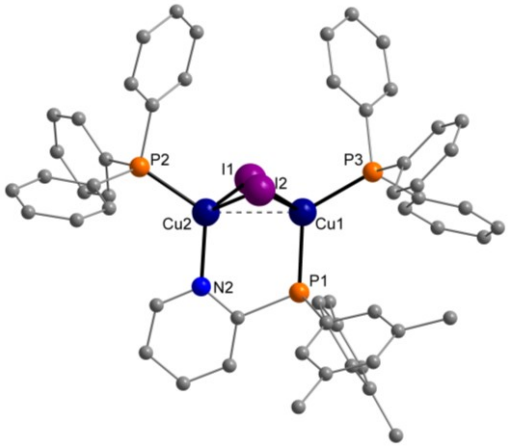

Figure 2. Molecular structure of **Cu-3a-H**. Hydrogen atoms and solvent molecules were omitted for clarity.

Also with the additional substituents, the well-known Cu_2I_2 butterfly-shaped metal halide core structure was formed.[20, 66, 68-70] **Table 1** gives selected molecular structural parameters of the bond lengths and angles of most of the dinuclear Cu(I) complexes. Besides the important Cu···Cu distance in the dinuclear complexes, also the bond length between Cu1 and P1 was of great interest, in order to verify whether the substituents have an impact. The shortest Cu···Cu distances were found for **Cu-1a-Furyl** with 2.68 Å and for **Cu-1a-F** with 2.71 Å. The average value for the Cu···Cu distance was 2.75 Å and in the same range as the Cu···Cu distances for the literature known PyrPhos copper compounds.[20, 66] The Cu1-P1 bond length did not change as a result of substituents on the phosphine moiety, 2.24 Å to 2.26 Å were found. Not even the fluorine atoms in complex **Cu-6a-H** (**Figure 6**) had an influence on the Cu1-P1 bond length.

Interestingly, the combination of the NP-bridging ligand **3b** and tris(4-fluorophenyl)phosphine **F** as ancillary ligand in a Cu(I) complex led to the formation of a tetranuclear species (**Cu-3b-F-4**) in most of the crystallization experiments which was not described in the literature before. This tetranuclear Cu(I) complex, $Cu_4I_4LP_3$, consists of one bidentate bridging ligand and three *para*-fluorinated triphenylphosphine ligands (compare **Figure 7** and ESI **Figure S70**). The four copper iodide units can be subdivided in two connected Cu_2I_2 butterfly shaped cores, one hold by the bridging ligand **3b** and one phosphine **F** and the other Cu_2I_2 copper iodide part coordinated by one tris(4-fluorophenyl)phosphine on each copper atom.

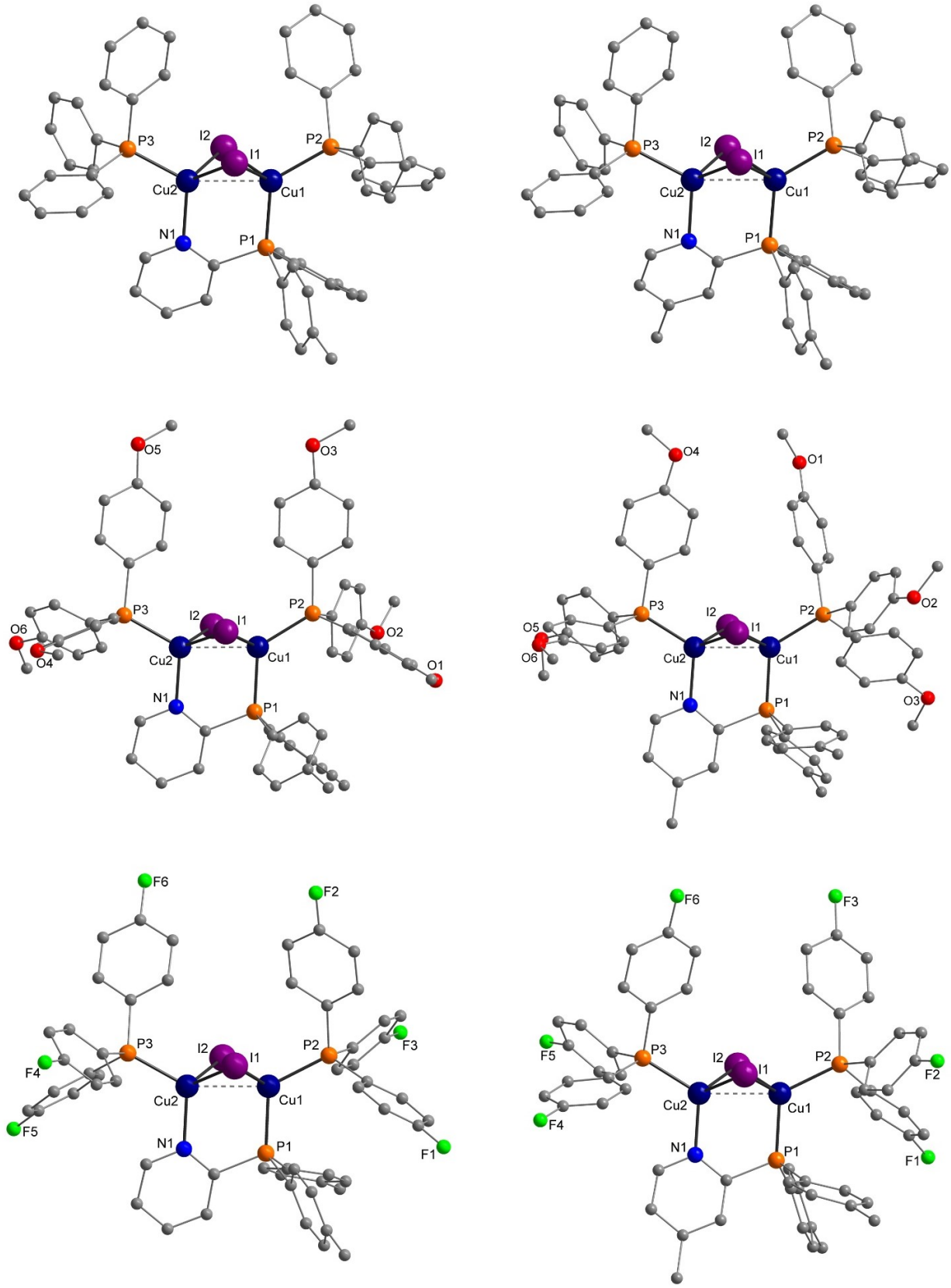

Figure 3. Molecular structures of the complexes **Cu-1a-H** (top, left), **Cu-1b-H** (top, right), **Cu-1a-MeO** (middle, left), **Cu-1b-MeO** (middle, right) and **Cu-1a-F** (bottom, left), **Cu-1b-F** (bottom, right), all bridged by the methylated phosphine ligands. Hydrogen atoms and solvent molecules were omitted for clarity.

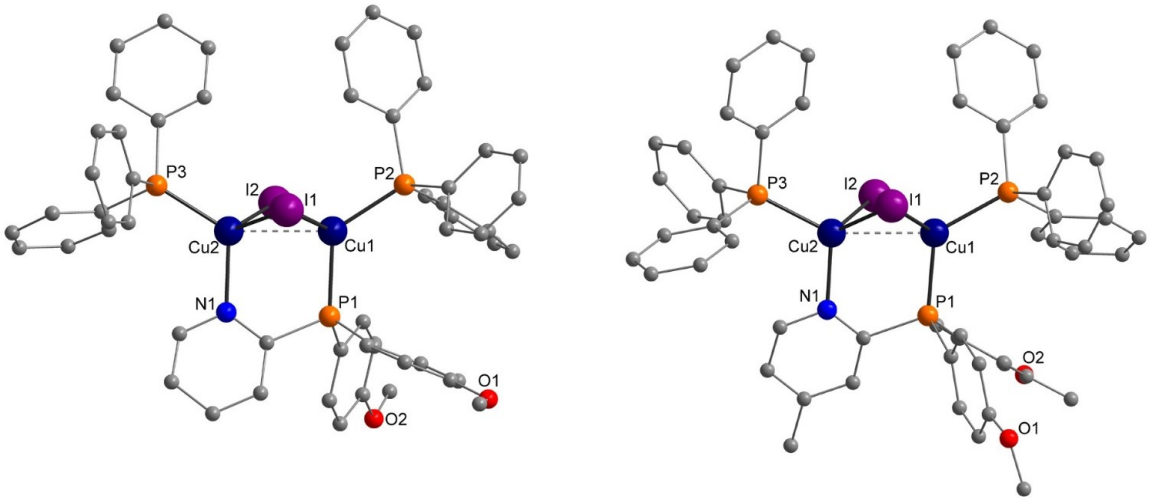

Figure 4. Molecular structures of the complexes **Cu-2a-H** (left) and **Cu-2b-H** (right) including *para*-di(methoxyphenyl)phosphinopyridine and its methylated derivate. Hydrogen atoms and solvent molecules were omitted for clarity.

Table 1. Selected parameters of the crystallographic data of the dinuclear copper complexes with a functionalized phosphine moiety of the NP-bridging ligands. Lengths are given in Å and angels are given in °.

	Cu-1a-H	**Cu-1b-H**	**Cu-1a-MeO**	**Cu-1b-MeO**	**Cu-1a-F**	**Cu-1b-F**
lengths						
Cu-Cu	2.7617(7)	2.7660(5)	2.7318(7)	2.7128(12)	2.7067(8)	2.7189(8)
Cu1-I	2.7160(6)	2.6834(4)	2.7021(6)	2.6570(9)	2.6597(9)	2.6697(6)
	2.6700(6)	2.7223(4)	2.6495(6)	2.6730(10)	2.6819(9)	2.6558(6)
Cu1-P1	2.2449(11)	2.2521(9)	2.2588(10)	2.2565(16)	2.2365(9)	2.2486(11)
Cu2-N1	2.127(3)	2.114(3)	2.103(3)	2.089(5)	2.096(2)	2.078(3)
Cu2-P3	2.2518(11)	2.2518(9)	2.2491(10)	2.2387(16)	2.2522(9)	2.2459(11)
Cu1-P2	2.2580(11)	2.2596(9)	2.2544(10)	2.2524(16)	2.2437(9)	2.2498(11)
angles						
Cu-I-Cu	61.727(16)	61.605(11)	61.453(17)	61.26(3)	61.153(16)	60.177(18)
	61.845(17)	61.970(12)	60.981(17)	60.72(3)	60.013(19)	61.422(18)
P-Cu-P	123.07(4)	124.16(3)	123.87(4)	124.28(7)	118.93(3)	119.01(4)

	Cu-1a-Furyl	**Cu-2a-H**	**Cu-2b-H**	**Cu-5a-H**	**Cu-5b-H**	**Cu-6a-H**
lengths						
Cu-Cu	2.6835(5)	2.7276(16)	2.7859(5)	2.7830(8)	2.7682(6)	2.7218(7)
Cu1-I	2.6513(4)	2.6786(12)	2.7129(4)	2.6645(7)	2.6608(5)	2.6698(5)
	2.6871(4)	2.7000(12)	2.6731(4)	2.6606(7)	2.6807(5)	2.7147(6)
Cu1-P1	2.2538(6)	2.241(2)	2.2523(6)	2.2400(11)	2.2381(9)	2.2499(9)
Cu2-N1	2.0720(19)	2.135(7)	2.1002(19)	2.076(4)	2.088(3)	2.116(3)
Cu2-P3	2.2293(6)	2.254(2)	2.2554(7)	2.2493(12)	2.2446(8)	2.2568(9)
Cu1-P2	2.2404(7)	2.245(2)	2.2583(7)	2.2526(11)	2.2503 (9)	2.2514(9)
angles						
Cu-I-Cu	59.851(11)	60.91(4)	62.428(11)	63.069(19)	62.530(14)	60.719(15)
	60.396(11)	60.81(4)	62.058(11)	61.944(19)	62.099(14)	61.000(15)
P-Cu-P	124.16(3)	124.78(9)	122.53(3)	120.27(4)	124.51(3)	123.26(3)

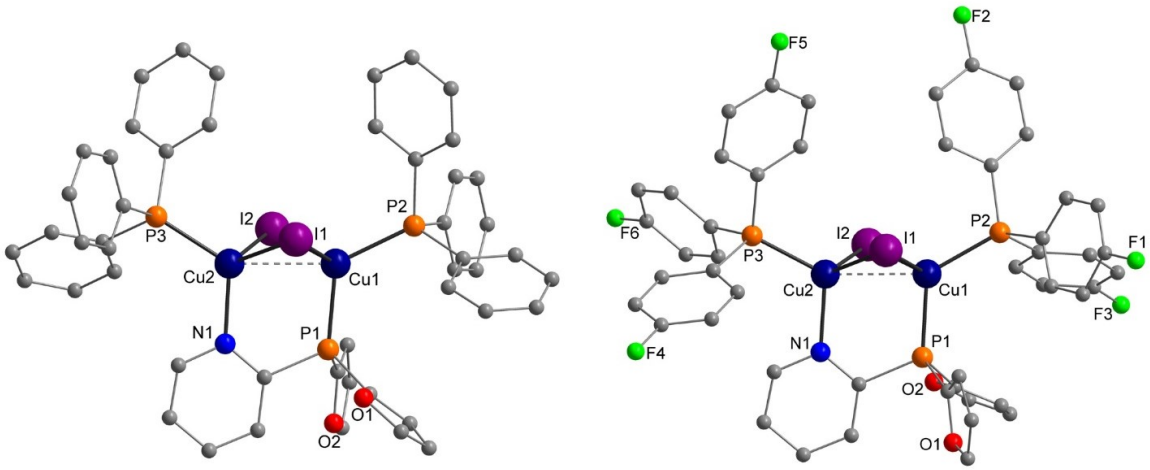

Figure 5. Molecular structures of complexes **Cu-5a-H** (left) and **Cu-5a-F** (right) bearing 2-furyl groups on the phosphine of the bridging ligand. Hydrogen atoms and solvent molecules were omitted for clarity.

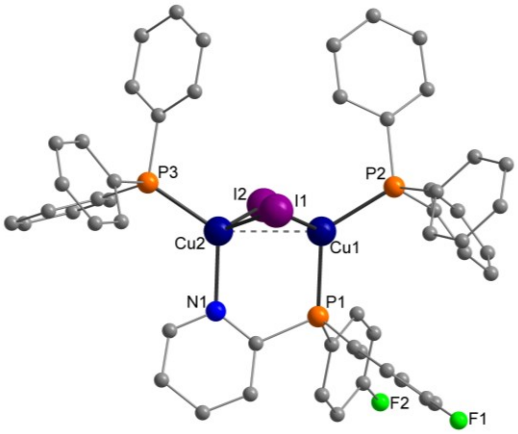

Figure 6. Molecular structure of **Cu-6a-H**. Hydrogen atoms and solvent molecules were omitted for clarity.

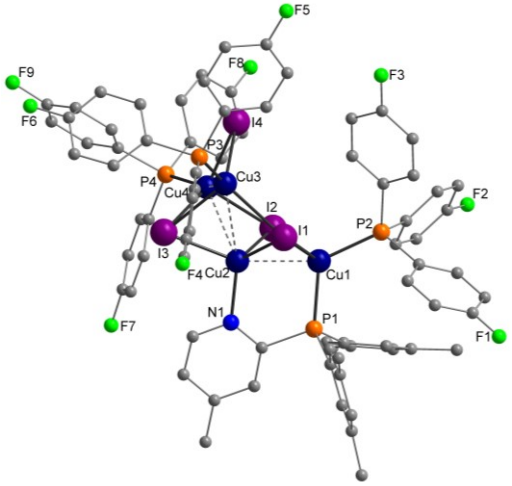

Figure 7. Tetranuclear structure $Cu_4I_4LP_3$, bearing ligand **3b** and tris(4-fluorophenyl)phosphine **F** (**Cu-3b-F-4**).

The Cu-I-Cu wings formed by the outer only **F**-coordinated copper halides are more opened with a wider I-Cu-I angle (109.38 ° for I4-Cu3-I3 and 109.17 ° for I4-Cu4-I3) compared to the other Cu_2I_2 NP-connected butterfly motif (only 106.02 ° for I1-Cu1-I2 and 105.95 ° for I1-Cu2-I2). The Cu···Cu distance with 2.67 Å for Cu1-Cu2 is in the common range compared to the di- and symmetric tetranuclear PyrPhos complexes, while the Cu3-Cu4 distance with 2.86 Å is a bit longer. The Cu_2I_2 unit built between Cu3 and Cu4 is only connected *via* one copper atom to the other Cu2I2 unit. The Cu2-Cu3 and Cu2-Cu4 distances are rather large with 3.01 Å and 2.86 Å, respectively. In case tetranuclear copper complexes are formed during crystallization, the growth of these crystals is probably favored over dinuclear species due to lower solubility of the tetranuclear complex. However, this was the only example where such a tetranuclear species was crystallized and the structure of the dinuclear Cu(I) complex **Cu-3b-F** could be proved by single crystal X-ray diffraction analysis (**Figure S69** and compare also **Table S1** for supplementary crystallographic data).

Quantum chemical calculations

For a better understanding of the electronic nature of the dinuclear Cu(I) complexes hold by bidentate phosphino-modified NP-ligands quantum computations were done. In **Figure 8** the frontier orbital HOMO (highest occupied molecular orbital) and LUMO (lowest unoccupied molecular orbital) plots as well as the spin density are shown for the benchmark complex **Cu-1b-H** with the triple of methyl groups on the bridging ligand.

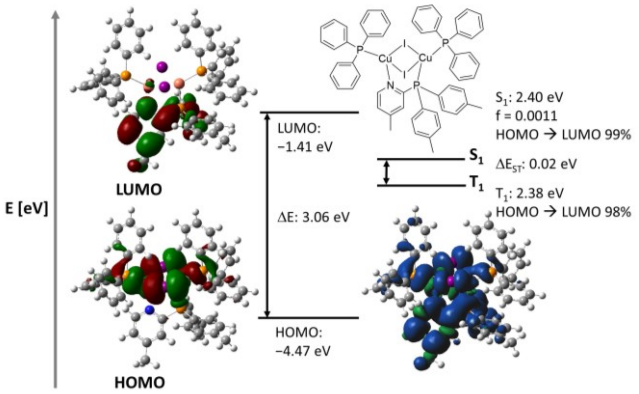

Figure 8. Overview of the HOMO and LUMO (left) and spin density (bottom, right) of Cu(I) complex **Cu-1b-H**.

As for all the other complexes, the HOMO (–4.47 eV) was located on the copper iodide core and partially on the phosphorus atoms of the ancillary ligands while the LUMO (–1.41 eV) spread over the NP-bridging ligand. The $\Delta E_{(HOMO-LUMO)}$ gap of complex **Cu-1b-H** had an average value for this class of complexes (3.06 eV, **Table 2**).

Table 2. HOMO and LUMO, $\Delta E_{(HOMO-LUMO)}$ gap and ΔE_{ST} gap values. All values are given in eV.

Complexes	HOMO [eV]	LUMO [eV]	ΔE [eV]	ΔE_{ST} [eV]
Cu-1a	–4.49	–1.49	2.99	0.03
Cu-1a-H	–4.51	–1.49	3.02	0.03
Cu-1b-H	–4.47	–1.41	3.06	0.02
Cu-1a-MeO	–4.29	–1.35	2.94	0.03
Cu-1b-MeO	–4.30	–1.25	3.05	0.03
Cu-1a-Furyl	–4.57	–1.43	3.14	0.03
Cu-1a-F	–4.79	–1.66	3.13	0.03
Cu-2a-H	–4.49	–1.42	3.07	0.03
Cu-2b-H	–4.46	–1.35	3.10	0.03
Cu-3a-H	–4.51	–1.46	3.05	0.03
Cu-3b-H	–4.48	–1.39	3.09	0.03
Cu-3b-F	–4.76	–1.57	3.19	0.03
Cu-4a-H	–4.52	–1.47	3.05	0.03
Cu-4b-H	–4.49	–1.37	3.13	0.03
Cu-5a-H	–4.55	–1.44	3.10	0.03
Cu-5a-F	–4.87	–1.68	3.18	0.03
Cu-5b-H	–4.51	–1.33	3.18	0.03
Cu-6a-H	–4.65	–1.65	2.99	0.02

The nature of the transitions in **Cu-1b-H** were based on HOMO and LUMO only, corresponding to exclusively metal- and halide-to-ligand charge transfer (MXLCT). The calculated energy of the singlet state S_1 with 2.40 eV and the calculated energy of the triplet state T_1 with 2.71 eV (calculated for 5 T states) resulted in a very small ΔE_{ST} gap of 0.02 eV without any other triplet states between this gap, allowing emission *via* the thermally activated delayed fluorescence pathway. The average value of the distance between the first singlet and first triplet state was 0.03 eV considering all complexes in this study.

An overview of all HOMO and LUMO levels as well as the $\Delta E_{(HOMO-LUMO)}$ gap and the ΔE_{ST} gap values for the multitude of copper complexes based on the novel NP-bridging ligands of this study is given in **Table 2**. Even though complexes **Cu-4a-H** and **Cu-4b-H** were synthetically not accessible, the calculated values are in a similar range as for the other copper complexes.

All things considered, the substituents on the phosphine moiety of the connecting NP-ligand in the Cu(I) complexes had no big influence on the electronic properties of the complexes. The effect of the *para*-methyl group on the pyridine ring slightly lowering the LUMO energy level (around –1.3 eV for **series b**), was more dominant than the influence of the phosphorus connected substituents (around –1.4 eV for **series a**).

Absorption spectra

The UV-vis absorption of the substituted phosphinopyridine bridged Cu(I) complexes was studied in dichloromethane at ambient temperature (**Figure 9** for Cu(I) complex **series a** and **Figure 10** for Cu(I) complex **series b**).

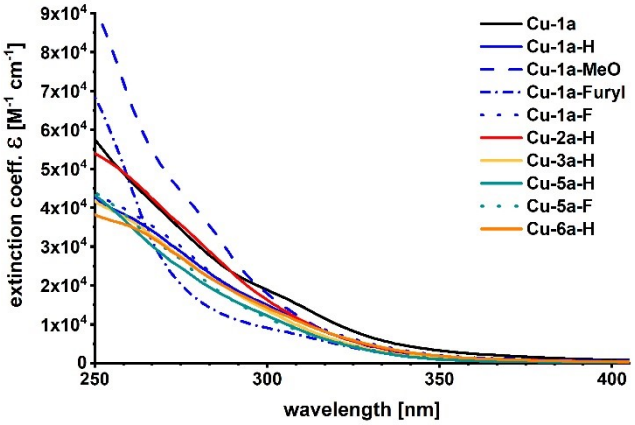

Figure 9. Absorption spectra of Cu(I) complex **series a** in dichloromethane (8×10^{-6} M) at 25 °C.

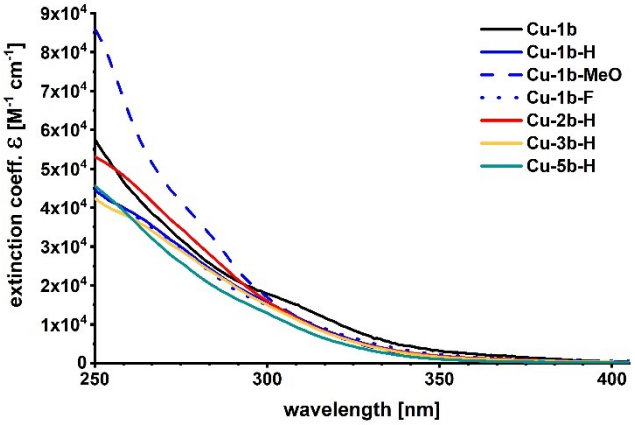

Figure 10. Absorption spectra of Cu(I) complex **series b** in dichloromethane (8×10^{-6} M) at 25 °C.

The UV-vis spectra were plotted as the resulting molar extinction coefficients. All absorption maxima were found at 250 nm due to the broadness of the spectra. Comparing all UV-vis spectra the extinction coefficient was in the same range around 4×10^4 M^{-1} cm^{-1} for most of the complexes and only slightly higher for the homoleptic complexes **Cu-1a** and **Cu-1b** as well as for the methoxy group bearing complexes **Cu-2a-H** and **Cu-2b-H**. The highest extinction coefficients were found for the two complexes **Cu-1a-MeO** and **Cu-1b-MeO** bearing tris(4-methoxyphenyl)phosphine and for complex **Cu-1a-Furyl** with tris(2-furyl)phosphine as ancillary ligand. In accordance with previous findings, tris(4-fluorophenyl)phosphine **F** had almost no impact on the extinction coefficients.[66]

The trends of the UV-vis spectra were in accordance to the prior described spectra of the well-known PyrPhos family (Cu(I) complexes based on 2-(dipenylphosphino)pyridine (PyrPhos) and derivatives).[18, 20, 26, 66]

Except for the *para*-methoxy groups, the substituents on the phosphine moiety of the NP-bridging ligand had almost no influence on the absorption of the corresponding dinuclear Cu(I) complexes.

For a better overview the Cu(I) complexes of **series 1a** and **series 1b** are also plotted separately in the ESI (**Figure S112** and **Figure S113**). Absorption spectra of the copper complexes in neat films can be also found in the ESI (**Figure S114** and **Figure S115**) and showed similar trends as in dichloromethane. The copper complexes bearing **MeO** as ancillary ligands exhibit an absorption among the highest absorptions of the whole class of copper complexes. In contrast to the spectra in dichloromethane, the absorption maxima of the copper complexes were found in the range of 250 nm to 270 nm. The complexes **Cu-1a-Furyl** and **Cu-1b-MeO** showed a second broad absorption band around 300 nm and 310 nm, respectively. These bands can be assigned to MXLCT.

Photophysical properties

Hereafter, the photophysics of this new class of Cu(I) complexes based on phosphine-modified NP-bridging ligands is reported of the powder samples as well as in doped films (20 wt% of the Cu(I) complexes in poly(methylmethacrylate) (PMMA) and CBP:TcTa (7:3) (with CBP = 4,4′-bis(*N*-carbazolyl)-1,1′-biphenyl and TcTa = 4,4',4"-tris(carbazol-9-yl)triphenylamine); the conditions for the film preparation are given in the ESI, chapter 7). **Table 3** shows the photophysical data obtained of the powders at ambient temperature with an excitation wavelength of 350 nm.

Table 3. Overview of the photophysics of the Cu(I) complexes as powder samples, measured with an excitation wavelength of 350 nm at ambient temperature and at 77 K given in brackets.

Copper Complex	Φ_{PL} [%]	λ_{PL} [nm]	τ [µs]	CIE X	CIE Y
Cu-1a	42	555	8.1 (56.0)	0.42	0.54
Cu-1b	42	551	8.0 (–)	0.42	0.53
Cu-1a-H	74	549	6.3 (40.0)	0.41	0.55
Cu-1b-H	83	531	6.5 (44.2)	0.34	0.55
Cu-1a-MeO	45	567	6.5 (50.7)	0.34	0.55
Cu-1b-MeO	61	556	8.7 (56.4)	0.42	0.53
Cu-1a-Furyl	67	524	6.8 (34.9)	0.32	0.52
Cu-1a-F	89	529	7.3 (56.5)	0.34	0.55
Cu-1b-F	85	520	6.9 (59.1)	0.30	0.53
Cu-2a-H	87	530	6.1 (72.8)	0.34	0.54
Cu-2b-H	76	538	7.3 (36.8)	0.37	0.54
Cu-3b-H	59	543	7.7 (58.7)	0.39	0.54
Cu-3b-F	70	540	9.6 (51.6)	0.38	0.54
Cu-5a-H	68	552	4.4 (24.2)	0.42	0.54
Cu-5b-H	68	520	5.5 (26.0)	0.31	0.52
Cu-5a-F	62	538	7.6 (45.9)	0.37	0.54
Cu-6a-H	61	561	7.3 (26.7)	0.43	0.54

Complex **Cu-1b-H** showed one of the highest photoluminescence quantum yields (PLQYs) in powder with 83%. The additional methyl groups on the phosphine moiety of the bridging ligand as well as the additional methoxy groups (**Cu-2a-H** 87% and **Cu-2b-H** 76%) influenced positively the PLQY compared to the other complexes of this study. In comparison, the PLQYs of the homoleptic complexes **Cu-1a** and **Cu-1b** were rather low and therefore only studied with the ligands **1a** and **1b** as a reference to the heteroleptic complexes.

The emission wavelengths of the investigated complexes were found in a range between 520 nm for complexes **Cu-1b-F** and **Cu-5b-H** and up to 561 nm for complex **Cu-6a-H** with two additional fluorine atoms on the phosphine moiety of the NP-ligand (**Table 3** and ESI **Figures S121** to **S122**). Probably the blue-shifting effect of the *para*-methyl group on the pyridine ring of the bridging ligands of the **series b** is dominant over the influence of the phosphorus bound groups (compare DFT section). The emission wavelengths for the class of copper complexes presented in this study in general are slightly red-shifted (5 nm to 10 nm) compared to the literature known copper complexes with NP-bridging ligands unsubstituted on the phosphine moiety **Cu-a-H** (514 nm[19]) and **Cu-b-H** (515 nm[19] and 510 nm[38]).

Comparing the excited state lifetimes of the Cu(I) complexes in solid phase, values between 4.4 µs and 8.1 µs were measured (**Table 3** and ESI **Figures S133** to **S141**). The complexes **Cu-5a-H** (4.4 µs) and **Cu-5b-H** (5.5 µs) with two 2-furyl groups on the phosphorus atom of the NP-ligand showed the shortest lifetimes. The lifetimes of all complexes are only slightly higher compared to the well-known complexes **Cu-a-H** (2.8 µs[19]) and **Cu-b-H** (3.8 µs[19] and 1.9 µs[38]) and therefore in the same microsecond range as described previously.[66] The small values in the microsecond range for the lifetime are an indication for TADF as the emission pathway.[40] Additionally, the lifetimes of the excited states were determined at 77 K of the powder samples (**Table 3** and ESI **Figures S142** and **S143**). The values for the lifetime were in average six to seven times higher at low temperatures compared to ambient temperature (6.5 µs to 44.2 µs at 77 K for complex **Cu-1b-H**). This is an indication for an emission as phosphorescence and a suppression of the temperature dependent reverse intersystem crossing (RISC) at 77 K.

The photophysics were also determined of doped PMMA (**Table 4**) and CBP:TcTa (7:3) films (**Table 5**) to exclude concentration and packing effects that may occur in the powder samples. For these studies the focus was placed on the Cu(I) complexes bearing triphenylphosphine **H** as ancillary ligands and the homoleptic complexes with the NP-ligands **1a** and **1b**, respectively.

In both host materials the PLQYs were found to have lower values compared to the measurements of the powders due to matrix effects. The PLQY values ranged from 33% to 57% (**Cu-5a-H** and **Cu-3b-H** in CBP:TcTa (7:3) respectively). Complex **Cu-1b-H** still showed one of the highest PLQYs in PMMA (55%) and in CBP:TcTa (7:3) (54%). Comparably high PLQYs were found for the complexes with methoxy

groups on the NP-bridging ligands and are in agreement with the trend observed of the powder samples. The photophysical properties of the two homoleptic Cu(I) complexes **Cu-1a** and **Cu-1b** that possessed the lowest PLQYs of the powder measurements were almost not affected by the host materials (42% PLQY in powder for both complexes, 38% and 42% in PMMA as well as 39% and 40% in CBP:TcTa (7:3), respectively).

Table 4. Overview of the photophysics of the Cu(I) complexes (20 wt%) in PMMA, measured with an excitation wavelength of 350 nm at ambient temperature.

Copper Complex	Φ_{PL} [%]	λ_{PL} [nm]	λ_{PL}[a] [nm]	τ [µs]	CIE X	CIE Y
Cu-1a	38	556	486	10.1	0.43	0.55
Cu-1b	42	541	516	11.8	0.37	0.52
Cu-1a-H	48	554	474	9.5	0.42	0.54
Cu-1b-H	55	540	490	10.4	0.37	0.53
Cu-2a-H	47	556	396	8.8	0.74	0.27
Cu-2b-H	53	541	490	10.4	0.37	0.54
Cu-3b-H	49	541	474	11.1	0.38	0.54
Cu-5a-H	40	555	476	10.0	0.42	0.53
Cu-5b-H	41	545	470	9.6	0.39	0.54
Cu-6a-H	42	555	466	9.0	0.42	0.55

[a] maxima of the photoluminescence spectra measured at 77 K

Table 5. Overview of the photophysics of the Cu(I) complexes (20 wt%) in CBP:TcTa (7:3), measured with an excitation wavelength of 350 nm at ambient temperature.

Copper Complex	Φ_{PL} [%]	λ_{PL} [nm]	τ [µs]	CIE X	CIE Y
Cu-1a	39	560	31.3	0.43	0.53
Cu-1b	40	549	17.6	0.41	0.53
Cu-1a-H	53	558	13.2	0.43	0.53
Cu-1b-H	54	548	33.5	0.40	0.54
Cu-2a-H	52	556	33.5	0.43	0.53
Cu-2b-H	53	549	31.3	0.40	0.54
Cu-3b-H	57	547	32.0	0.40	0.54
Cu-5a-H	33	560	5.7	0.44	0.52
Cu-5b-H	45	540	12.1	0.38	0.52
Cu-6a-H	47	561	28.3	0.43	0.52

Using PMMA as host material, the excited state lifetimes of the Cu(I) complexes were only minimal longer (2 µs to 4 µs and 6 µs for complex **Cu-5a-H**) compared to the values of the powders (**Table 4** and ESI **Figures S144** to **S148**). The CBP:TcTa (7:3) matrix increased the excited state lifetimes drastically by two and up to five times in comparison to the powders and PMMA films (**Table 5** and ESI **Figures S149** to **S153**).

The doped films showed a more defined trend for the emission wavelengths in contrast to the values of the powder measurements (**Table 3** to **5** and ESI **Figures S124** to **S132**). The different substituents around the phosphorus atom of the bridging ligand had no influence on the photoluminescence. 555 nm and values close to this one were determined for the maxima of the photoluminescence spectra for all investigated complexes without an additional substituent on the pyridine (**series a**), while the additional methyl group in *para*-position of the pyridine moiety (**series b**) induced a significant hypsochromic-shift of up to 15 nm in the PMMA films at ambient temperature with an excitation wavelength of 350 nm. The homoleptic complexes **Cu-1a** and **Cu-1b** showed a very slight red-shift compared to their related triphenylphosphine heteroleptic complexes **Cu-1a-H** and **Cu-1b-H** in PMMA films.

Similar observations were made for the films with CBP:TcTa (7:3). In general, the emission wavelengths of these films were only slightly bathochromic-shifted compared to the PMMA films.

Low temperature photoluminescence measurements (77 K) of the doped PMMA films were performed to further investigate the mechanism of the emission pathway (**Table 4**, ESI **Figures S127** to **S129**). Usually, a bathochromic-shift at low temperatures is observed for Cu(I) complexes in the solid state possessing TADF due to an energetically hindered RISC and a resulting emission from the lowest triplet state as phosphorescence.[26, 40, 66] The emission maxima of the Cu(I) complexes in PMMA in this study showed a hypsochromic-shift at 77 K compared to the emission spectra recorded at ambient temperature. This unexpected blue-shift corresponds with the lack of stabilization of the Cu(I) complexes in the PMMA matrix at low temperatures upon excitation. This phenomenon is widely known for the photoluminescence of Cu(I) complexes studied in solution at various temperatures.[31, 71-74] At 77 K the Cu(I) complexes are encapsulated in a rigid matrix leading to structures of higher energy and therefore a blue-shift of the emission. For a few dinuclear Cu(I) complexes of the composition $Cu_2I_2L_3$ a blue-shift at 77 K was observed of the powder samples in a study by Zink and coworkers.[69] Rigidochromic effects, including a destabilization of the emissive state at 77 K due to greater rigidity and an overcompensation of the potential red-shift, expected for the TADF process, were discussed. Therefore, the most plausible reason for the hypsochromic-shift at 77 K in PMMA films of this present work are rigidochromic effects and that these effects prevail over electronic effects induced by TADF. Kobayashi and coworkers described a similar blue-shift of the emission as phosphorescence at low temperatures for the pure organic TADF emitter 4CzIPN in doped films and explained it with a four-level model involving the states S_1, T_1, T_n and S_0.[75] In this model the additional triplet excited state T_n is located energetically between the two lowest excited states T_1 and S_1. An additional involved T_n state as well as an inversion of the singlet-triplet gap[76, 77] cannot be excluded a priori. Thus, the lowest excited states will be studied with other methods than TDDFT in upcoming projects.

OLED devices

Finally, a multitude of OLED devices with the Cu(I) complexes bearing the phosphino-modified NP-bridging ligands were prepared and tested.

In order to select the material of the OLED auxiliary layers purposefully, the energy of the HOMO and LUMO levels of the complexes were determined first. For this the photoemission yield spectroscopy (PYS) method in combination with absorption spectroscopy (compare ESI, chapter 6) was applied. Firstly, the HOMO energy of the materials was determined by using the PYS method. Then the HOMO-LUMO energy gap (E_g) was calculated with the help of the absorption band and then the LUMO energy value was obtained using the inverse formula.

$$LUMO = HOMO - E_g.$$

For the testing in OLED devices almost all obtained copper complexes were inserted into the device within the same heterostructure ITO (120-160 nm) / PEDOT:PSS (50 nm) / poly-TPD (15 nm) / **20 wt% emitter:host** (20 nm) / TPBi (30 nm) / LiF (1 nm) / Al (>100 nm) (with ITO = indium tin oxide, PEDOT:PSS = poly(3,4-ethylenedioxythiophene): poly(styrenesulfonate), poly-TPD = poly(4-butyltriphenylamine and TPBi = 2,2′,2"-(1,3,5-benzinetriyl)-tris(1-phenyl-1-*H*-benzimidazol), **Figure 11**).

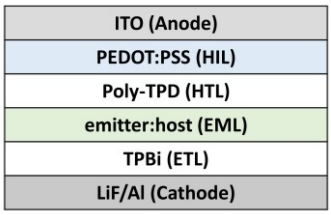

Figure 11. OLED stack architecture used for most of the devices. The actual layer thickness was not taken into account in this overview of the layers.

As host material either CBP, CBP:TcTa or DMFL-CBP (2,7-bis(carbazol-9-yl)-9,9-dimethylfluorene) were used (ESI, **Table S4** and **Figure 12**, **Figure 13**). The starting point for the host material optimization was CBP. CBP is a well-known bipolar host material[78-80] and it was demonstrated before that high quality films of CBP could be deposited from solution.[81, 82]. Zhang and coworkers showed that CBP doped with TcTa in a 7:3 ratio led to a significant increase of the device efficiency.[78]

Poly-TPD was chosen as hole transport layer due to its insolubility in most solvents after post-treatment (annealing at 220 ºC for 30 min in an argon-glovebox).[83] As electron transport layer (ETL) and hole transport layer (HTL) the well-known and often used TPBi and PEDOT:PSS materials were selected.[51, 55, 84, 85] Assuming similar properties of the selected copper emitters, the best host material was chosen by the comparison of the performance of a series of OLED devices based on Cu(I) complex emitter **Cu-1b-H** in various host materials.

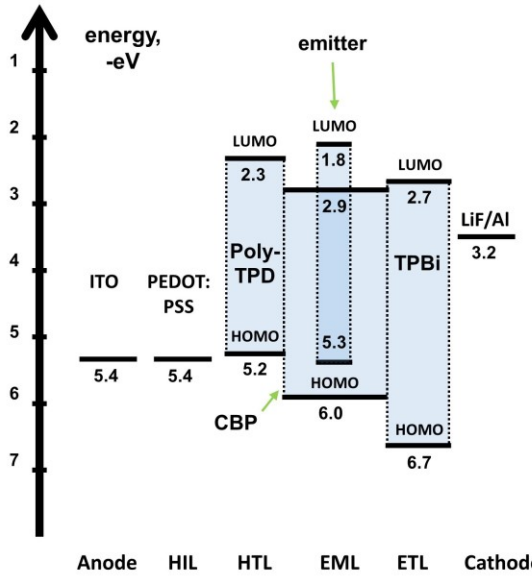

Figure 12. Overview of the energy levels of the obtained OLED device with **Cu-1b-H** (20 wt%) and CBP as host material in the EML (OLED1).

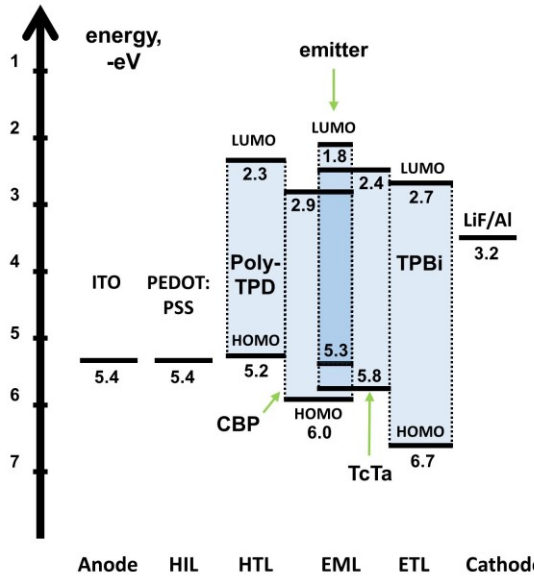

Figure 13. Overview of the energy levels of the obtained OLED device with **Cu-1b-H** (20 wt%) and CBP:TcTa (7:3) as host material in the EML (OLED3).

Since OLED3 (CBP:TcTa (7:3)) demonstrated the highest efficiency among OLED1 (CBP) and OLED30 (DMFL-CBP), CBP:TcTa (7:3) was selected as host material. The HOMO-LUMO levels of CBP:TcTa matched best with those of the copper emitter **Cu-1b-H** so that the holes and electrons recombine almost exclusively in the emitter molecules. In conclusion all copper emitter materials were tested in the heterostructure ITO (120-160 nm) / PEDOT:PSS (50 nm) / poly-TPD (15 nm) / **20 wt% emitter:CBP:TcTa (7:3)** (20 nm) / TPBi (30 nm) / LiF(1 nm) / Al (>100 nm), in which the emitter material was **Cu-1a** to **Cu-6a-H** (compare ESI). To enable a proper comparison of the performance of the obtained OLED devices, the electroluminescence (EL) spectra were measured at the same conditions,

only the integration time was varied when measuring the EL intensity. Thus, the intensity is given in sec^{-1}, which corresponds to the counts divided by the integration time.

The best performance was demonstrated by OLED3 and OLED19 based on EMLs with **Cu-1b-H** and **Cu-6a-H** (**Figure 14** and **Figure 15**).

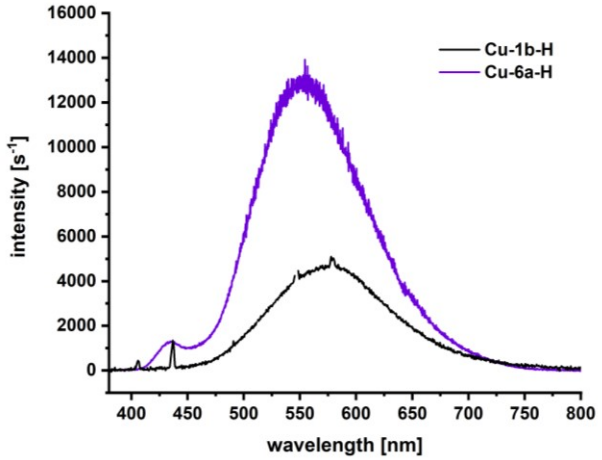

Figure 14. EL spectra of **Cu-1b-H** and **Cu-6a-H** (OLED3 and OLED19)

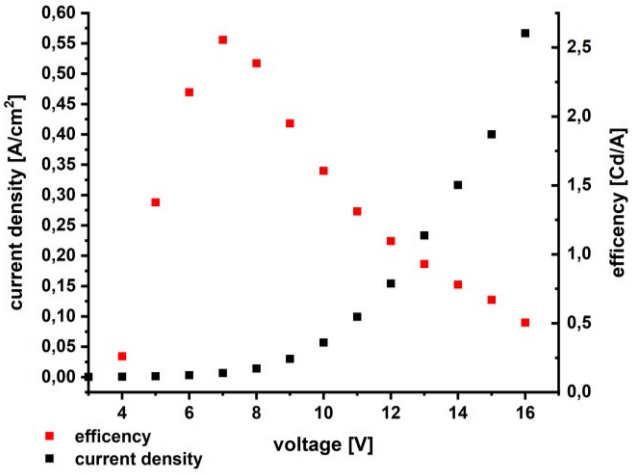

Figure 15. I-V curve and current efficiency for the OLED device with emitter **Cu-6a-H** (OLED19).

The brightness of the devices based on these two copper emitters reached 2300 Cd/m² and 2900 Cd/m² and the current efficiency up to 3.5 Cd/A and 2.4 Cd/A, respectively. For the devices based on the other Cu(I) complexes, brightnesses in the range of 350 Cd/m² up to 2200 Cd/m² was found. The current efficiencies of these OLED devices were in the range of 0.64 Cd/A to 5.27 Cd/A.

In order to achieve a maximum brightness, the OLED devices based on the best performing materials (EML with **Cu-1b-H** and **Cu-6a-H**) were further optimized. Firstly, the effect of the HTL thickness, which affects the charge carrier balance, was investigated. It turned out that a poly-TPD thickness of 15 nm (OLED3 with 2330 Cd/m²) demonstrated a higher brightness compared to a layer of 30 nm (OLED5 with 2080 Cd/m²). According to these results all further OLED devices were built with a fixed value of 15 nm for the HTL.

Secondly, different thicknesses of TPBi as the ETL were investigated. Also the influence of other ETL materials instead of TPBi was taken into account. As further ETL materials, OXD-7 (1,3-bis[2-(4-*tert*-butylphenyl)-1,3,4-oxadiazo-5-yl]benzol), Alq_3 (tris-(8-hydroxyquinoline)aluminium) and TAZ (3-(biphenyl-4-yl)-5-(4-*tert*-butylphenyl)-4-phenyl-4H-1,2,4-triazole), which are all well-known in the literature, were tested.[86] Unfortunately, the devices OLED17 (reduction of the TPBi layer from 30 nm to 15 nm) and OLED26-OLED28 (30 nm OXD-7, Alq_3 and TAZ respectively) showed a significant decrease of the luminescence brightness (see ESI). The same trend was found for the OLED devices based on the EML with **Cu-6a-H**.

Thirdly, the emission layer thickness was varied in order to decrease the turn-on-voltage and the charge carrier balance. The thickness of the EML was tuned by changing the spin-coater frequency rate. A frequency of 1060 rpm gave a 45 nm layer (OLED29), 1500 rpm resulted in 30 nm (OLED21) and with up to 2120 rpm a thinner EML of 15 nm (OLED22) was realized. The device with the thickest emission layer (OLED29) showed the lowest turn-on-voltage (4 V) and the highest brightness of up to 5900 Cd/m². In comparison to the photoluminescence of the Cu(I) complexes in doped films (20 wt% in CBP:TcTa (7:3)) at ambient temperature, the electroluminescence was slightly shifted while the curve progression was very similar (ESI **Figures S186** to **S190**). The observed shift is very small and can be explained by the generalized Stark effect[87-89] or partial reabsorption by the neighboring organic layers within the OLED heterostructure, absent when the photoluminescence was investigated.[90, 91] The electroluminescence originates from the Cu(I) complexes and not from the matrix, while for the photoluminescence a slight contribution from the matrix is visible. In general, the emission of the doped films and the corresponding OLEDs are comparable.

Since the efficiency of OLEDs is extremely sensitive to the cleanroom class, a further increase of the efficiency and brightness of the devices would have required other OLED manufacturing equipment up to professional level, which was unfortunately not accessible to us. This resulted in lower efficiencies of the obtained OLED devices relatively to the previously published results for the Cu(I) complexes of the same nature.[39] At the same time, the obtained brightness and efficiency are on the same level or above the values obtained for similar compounds in literature, which shows the advantages of the novel Cu(I) complexes in combination with the used stack architecture in the OLED device.[19, 46] The details of all fabricated OLEDs can be found in ESI **Table S3** and **S4** and I-V curves as well as the calculated current efficiencies are given in ESI **Figures S154** to **S185**.

All in all, the best OLED performance of this series of Cu(I) complexes with phosphino-modified NP-bridging ligands was demonstrated by OLED29 with the copper emitter **Cu-1b-H** bearing the triple methylated NP-bridging ligand with a high brightness of 5900 Cd/m² and a good current efficiency of 3.79 Cd/A.

CONCLUSION

A new class of dinuclear iodide bridged Cu(I) complexes of the PyrPhos family with *para*-substituted diphenylphosphinopyridine bridging ligands with the modification focus on the phosphine moiety of the NP-ligand was investigated in this work. The influence of this part of the bridging ligand was not studied intensively before. The resulting phosphino-modified NP-ligand bridged copper complexes in this study were completely characterized and tested in solution-processed organic light-emitting diodes afterwards. Almost all copper complexes as well as some of the ligands were fully pictured by single crystal X-ray diffraction analyses. The substituents on the phosphorus atom of the bridging ligands, ranging from 4-methylphenyl to 4-fluorophenyl over 2-furyl were all tolerated in the synthesis of copper complexes of the type $Cu_2I_2LP_2$. The different phosphine moieties had nearly no impact on the electronic properties of the complexes as found by quantum computational studies. As stated for other dinuclear $Cu(I)_2X_2$ complexes, the HOMO was located mostly on the copper halide core, while the LUMO spread out over the NP-bridging ligand. The best photophysical results in solid state were found for the complexes bearing the methylated bridging ligands (**Cu-1a-F** 89%, **Cu-1b-F** 85% and **Cu-1b-H** 83% PLQY) and the ones with methoxy groups (**Cu-2a-H** 87% PLQY) with emission wavelengths in the range between 520 nm and 561 nm for all complexes. The short excited state lifetimes with an average value of 6.9 µs and 4.4 µs for complex **Cu-5a-H** with 2-(bis(2-furyl)phosphino)pyridine indicate an emission pathway as thermally activated delayed fluorescence also for these Cu(I) complexes. The Cu(I) based emitters were investigated in several different heterostructures for OLED devices. The stack architecture of ITO / PEDOT-PSS (50 nm) / poly-TPD (15 nm) / 20 wt% Cu(I) emitter:CBP:TcTA (7:3) (45 nm) / TPBi (30 nm) / LiF(1 nm)/Al (>100 nm) was found to give the best properties. The optimized OLED device consisting of an EML with **Cu-1b-H** bearing the triple methylated NP-bridging ligand showed a high brightness of 5900 Cd/m² and a good current efficiency of 3.79 Cd/A (OLED29). All in all, the structural diversity of the Cu(I) complexes themselves as well as the different heterostructures of the OLED devices gave a multitude of design varieties.

EXPERIMENTAL

All chemicals used in this work for the synthesis of the ligands as well as for the copper complex synthesis, including solvents, precursors and further reactants, were purchased commercially from the common vendors (*Merck*, *Fisher*, *abcr* and *ChemPur*) and were used without further purification. Copper(I) iodide was purchased on trace metals basis (99.999%). All solvents in p.a. quality were used directly for extractions, column chromatography and the work up procedure of the copper complexes. Dry solvents were obtained with the SPS drying system of *MBraun*, model MB-SPS-800. For this drying system solvents in HPLC grade, mostly without a stabilizer, were used. All solvents tapped of the system were degassed with argon for 20 min prior to usage. All reactions in this study were performed under the general Schlenk conditions. For the complete characterization, all products were confirmed *via* NMR measurements. For this purpose eight inch NMR tubes with the sample and 0.5 mL of DMSO-d_6 for each tube were melted under air exclusion. The used DMSO-d_6 (≥ 99.80% D) was purchased from *Eurisotop* in 10 mL vials with a septum and were degassed with argon prior to use.

Synthesis of the *para*-substituted bridging ligands

The general synthesis procedures as well as the complete analytical characterization of the *para*-substituted diphenylphosphinopyridine bridging ligands can be found in the ESI.

All Cu(I) complexes in this study were prepared according to the following general procedure.

Synthesis of the Cu(I) complexes – general procedure

An established synthesis procedure for Cu(I) complexes was applied.[19, 20] For the copper complex production in this study, the corresponding phosphino-modified NP-bridging ligand (0.20 mmol up to 2.4 mmol, 1.00 eq.), the ancillary phosphine (0.40 mmol up to 4.8 mmol, 2.00 eq.) and copper iodide (0.40 mmol up to 4.8 mmol, 2.00 eq.) were suspended in 10 mL to 15 mL of dry and freshly with argon degassed dichloromethane (SPS). The reaction mixture was degassed for another 20 min with Ar. All reactions were stirred at 25 °C for 15 h. In case the reaction mixture was still a solution after the reaction time was over, the volume of the solution was at least reduced to half of the original volume and was added dropwise to an excess of *n*-pentane (100 mL up to 300 mL depending on the concentration and amount of the dichloromethane reaction mixture). Precipitates in different shades yellow were obtained, filtered off and washed with *n*-pentane (2 × 25 mL or more repetitions) and with diethylether (2 × 10 mL, sometimes in parallel with *n*-pentane, depending on the solubility of the resulting complex in diethylether). If the reaction resulted in a suspension, the volume of the solution part was reduced in some cases and then added to *n*-pentane as described above. Solvent residues in the obtained powders were removed under reduced pressure, yielding the target Cu(I) complexes in good to very high yields.

In the following H_L represents protons of the bridging ligands and H_P represents protons of the ancillary ligands of the complexes in each NMR part of the characterization. The same classification was used for the mass analysis (L = bridging ligand, P = ancillary ligand).

[(2-(Bis(4-methylphenyl)phosphino)pyridine)$_3$Cu$_2$I$_2$] (**Cu-1a**)

Complex **Cu-1a** was synthesized according to the general procedure and was obtained as a pale yellow powder (82% yield).

^{1}H NMR (400 MHz, DMSO-d_6) δ [ppm] = 8.96 (bs, 3H, $H_{L(Pyr)}$), 7.90 (t, $^3J_{HH}$ = 7.3 Hz, 3H, $H_{L(Pyr)}$), 7.56 (bs, 3H, $H_{L(Pyr)}$), 7.46 (d, $^3J_{HH}$ = 4.8 Hz, 3H, $H_{L(Pyr)}$), 7.16 (bs, 12 H, $H_{L(Tolyl)}$), 7.09 (d, $^3J_{HH}$ = 7.4 Hz, 12H, $H_{L(Tolyl)}$), 2.28 (s, 18H, $H_{L(Me)}$). – **^{13}C NMR** (101 MHz, DMSO-d_6) δ [ppm] = 151.0 (d, J_{CP} = 13.4 Hz), 139.8 (s), 137.5 (bs), 133.3 (d, J_{CP} = 13.4 Hz), 131.6 (d, J_{CP} = 9.7 Hz), 131.0 (d, J_{CP} = 12.4 Hz), 129.2 (d, J_{CP} = 7.8 Hz), 128.4 (d, J_{CP} = 30.0 Hz), 125.1 (bs), 20.9 (s, 6C, $C_{L(Me)}$). – **^{31}P NMR** (162 MHz, DMSO-d_6) δ [ppm] = –6.62 (bs, 3P, P_L). – **MS** (FAB, 3-NBA) *m/z* [%] = 1505 (1) $[Cu_4I_3L_3]^+$, 1315 (2) $[M+Cu]^+$, 1214 (8) $[Cu_4I_3L_2]^+$, 1126 (2) $[M–I]^+$, 1024 (23) $[Cu_3I_2L_2]^+$, 834 (26) $[Cu_2IL_2]^+$, 733 (24) $[Cu_3I_2L]^+$, 645 (42) $[CuL_2]^+$, 543 (55) $[Cu_2IL]^+$, 354 (100) $[CuL]^+$, 292 (12) $[L+H]^+$, 200 (11) [L–Tolyl]$^+$. – **IR** (ATR) $\tilde{\nu}$ [cm^{-1}] = 2916 (vw), 1571 (w), 1497 (w), 1449 (w), 1419 (w), 1187 (w), 1092 (w), 1020 (vw), 803 (w), 763 (w), 742 (w), 709 (w), 614 (w), 509 (m), 406 (w). – **Elemental anal.** calcd for $C_{57}H_{54}Cu_2I_2N_3P_3$ (1253.0): C 54.56, H 4.34, N 3.35; found: C 53.57, H 4.29, N 3.22.

[(2-(Bis(4-methylphenyl)phosphino)pyridine)(triphenylphosphine)$_2$Cu$_2$I$_2$] (**Cu-1a-H**)

Complex **Cu-1a-H** was synthesized according to the general procedure and crystallized from a mixture of DCM and *n*-pentane. The product was obtained as a pale yellow powder (97% yield).

^{1}H NMR (400 MHz, DMSO-d_6) δ [ppm] = 8.64 (bs, 1H, $H_{L(Pyr)}$), 7.90 (t, $^3J_{HH}$ = 7.5 Hz, 1H, $H_{L(Pyr)}$), 7.55 (bs, 1H, $H_{L(Pyr)}$), 7.46 – 7.33 (m, 31H, H_P, $H_{L(Pyr)}$), 7.20 (bs, 4H, $H_{L(Tolyl)}$), 7.08 (d, $^3J_{HH}$ = 7.8 Hz, 4H, $H_{L(Tolyl)}$), 2.29 (s, 6H, $H_{L(Me)}$). – **^{13}C NMR** (101 MHz, DMSO-d_6) δ [ppm] = 139.7 (s), 133.7 (d, J_{CP} = 13.9 Hz), 133.4 (d, J_{CP} = 14.3 Hz), 133.0 (d, J_{CP} = 28.3 Hz), 129.9 (s), 129.2 (d, J_{CP} = 7.7 Hz), 128.5 (d, J_{CP} = 8.3 Hz), 20.9 (s, 2C, $C_{L(Me)}$). – **^{31}P NMR** (162 MHz, DMSO-d_6) δ [ppm] = –5.91 (bs, 1P, P_L), –9.08 (bs, 2P, P_P). – **MS** (FAB, 3-NBA) *m/z* [%] = 1257 (2) $[M+Cu]^+$, 1214 (5) $[Cu_4I_3L_2]^+$, 1068 (6) $[M–I]^+$, 1024 (40) $[Cu_3I_2L_2]^+$, 995 (5) $[Cu_3I_2LP]^+$, 834 (18) $[Cu_2IL_2]^+$, 805 (38) $[Cu_2ILP]^+$, 776 (14) $[Cu_2IP_2]^+$, 733 (40) $[Cu_3I_2L]^+$, 645 (36) $[CuL_2]^+$, 616 (86) $[CuLP]^+$, 587 (87) $[CuP_2]^+$, 543 (100) $[Cu_2IL]^+$. – **IR** (ATR) $\tilde{\nu}$ [cm^{-1}] = 1479 (w), 1433 (w), 1188 (vw), 1157 (vw), 1093 (w), 1029 (vw), 999 (vw), 805 (w), 745 (m), 693 (m), 617 (w), 513 (m), 500 (m), 430 (w). – **Elemental anal.** calcd for $C_{55}H_{48}Cu_2I_2NP_3$ (1194.9): C 55.20, H 4.04, N 1.17; found: C 54.48, H 3.97, N 1.14. The molecular structure of the complex was determined by single crystal X-ray diffraction (CCDC 1996791).

[(2-(Bis(4-methylphenyl)phosphino)pyridin)(tris(4-methoxyphenyl)phosphine)$_2$Cu$_2$I$_2$] (**Cu-1a-MeO**)

Complex **Cu-1a-MeO** was synthesized according to the general procedure and crystallized from DCM and *n*-pentane. The product was obtained as a pale yellow powder (91% yield).

^{1}H NMR (400 MHz, DMSO-d_6) δ [ppm] = 8.65 (bs, 1H, $H_{L(Pyr)}$), 7.88 (t, $^3J_{HH}$ = 7.5 Hz, 1H, $H_{L(Pyr)}$), 7.57 (d, $^3J_{HH}$ = 7.4 Hz, 1H, $H_{L(Pyr)}$), 7.43 (bs, 1H, $H_{L(Pyr)}$), 7.37 – 7.33 (m, 12H, H_P), 7.24 (bs, 4H, $H_{L(Tolyl)}$), 7.09 (d, $^3J_{HH}$ = 7.8 Hz, 4H, $H_{L(Tolyl)}$), 6.89 (d, $^3J_{HH}$ = 8.4 Hz, 12H, H_P), 3.76 (s, 18H, $H_{P(MeO)}$), 2.29 (s, 6H, $H_{L(Me)}$). – **^{13}C NMR** (101 MHz, DMSO-d_6) δ [ppm] = 160.3 (s), 139.6 (s), 135.1 (d, J_{CP} = 14.9 Hz), 133.5 (d, J_{CP} = 12.9 Hz), 129.1 (d, J_{CP} = 7.7 Hz), 124.6 (d, J_{CP} = 32.8 Hz), 114.1 (d, J_{CP} = 8.9 Hz), 55.1 (s, 6C, $C_{P(MeO)}$), 20.9 (s, 2C, $C_{L(Me)}$). – **^{31}P NMR** (162 MHz, DMSO-d_6) δ [ppm] = –6.28 (bs, 1P, P_L), –13.10 (bs, 2P, P_P). – **MS** (FAB, 3-NBA) *m/z* [%] = 1437 (6) $[M+Cu]^+$, 1376 (1) $[M+H]^+$, 1248 (5) $[M–I]^+$, 1146 (2) $[Cu_3I_2P_2]^+$, 1085 (5) $[Cu_3I_2LP]^+$, 1024 (11) $[Cu_3I_2L_2]^+$, 997 (17) $[Cu_2IP_2]^+$, 896 (13) $[Cu_2ILP]^+$, 767 (65) $[CuP_2]^+$, 706 (100) $[CuLP]^+$, 543 (51) $[Cu_2IL]^+$, 415 (19) $[CuP]^+$, 354 (83) $[CuL]^+$, 353 (35) $[P+H]^+$, 292 (15) $[L+H]^+$. – **IR** (ATR) $\tilde{\nu}$ [cm^{-1}] = 2834 (vw), 1592 (m), 1568 (w), 1498 (m), 1456 (w), 1402 (vw), 1286 (w), 1247 (m), 1177 (m), 1097 (m), 1026 (m), 825 (m), 797 (m), 764 (w), 717 (vw), 615 (w), 520 (m), 450 (w), 417 (w). – **Elemental anal.** calcd for $C_{61}H_{60}Cu_2I_2NO_6P_3$ (1375.0): C 53.21, H 4.39, N 1.02; found: C 52.40, H 4.29, N 0.94. The molecular structure of the complex was determined by single crystal X-ray diffraction (CCDC 1996796).

[(2-(Bis(4-methylphenyl)phosphino)pyridine)(tri(2-furyl)phosphine)$_2$Cu$_2$I$_2$] (**Cu-1a-Furyl**)

Complex **Cu-1a-Furyl** was synthesized according to the general procedure and crystallized from DCM and *n*-pentane. The product was obtained as a pale yellow powder (86% yield).

^{1}H NMR (400 MHz, DMSO-d_6) δ [ppm] = 8.82 (bs, 1H, $H_{L(Pyr)}$), 7.96 (s, 6H, H_P), 7.93 (bs, 1H, $H_{L(Pyr)}$), 7.63 (d, $^3J_{HH}$ = 6.9 Hz, 1H, $H_{L(Pyr)}$), 7.55 (d, $^3J_{HH}$ = 6.5 Hz, 1H, $H_{L(Pyr)}$), 7.33 (bs, 4H, $H_{L(Tolyl)}$), 7.15 (d, $^3J_{HH}$ = 7.5 Hz, 4H, $H_{L(Tolyl)}$), 7.08 (bs, 6H, H_P), 6.55 (dt, $^3J_{HH}$ = 3.6 Hz, $^3J_{HH}$ = 1.9 Hz, 6H, H_P), 2.30 (s, 6H, $H_{L(Me)}$). – **^{13}C NMR** (101 MHz, DMSO-d_6) δ [ppm] = 151.4 (d, J_{CP} = 13.3 Hz), 148.8 (d, J_{CP} = 3.4 Hz), 144.8 (d, J_{CP} = 38.7 Hz), 139.9 (s), 138.0 (bs), 133.5 (d, J_{CP} = 13.8 Hz), 132.0 (bs), 129.3 (d, J_{CP} = 8.3 Hz), 128.7 (d, J_{CP} = 27.7 Hz), 125.2 (bs), 123.2 (d, J_{CP} = 26.0 Hz), 111.1 (d, J_{CP} = 8.1 Hz), 20.9 (s, 2C, $C_{L(Me)}$). – **^{31}P NMR** (162 MHz, DMSO-d_6) δ [ppm] = –4.98 (bs, 1P, P_L), –71.98 (bs, 2P, P_P). – **MS** (FAB, 3-NBA) *m/z* [%] = 775 (11) $[Cu_2ILP]^+$, 733 (19) $[Cu_3I_2L]^+$, 586 (9) $[CuLP]^+$, 543 (52) $[Cu_2IL]^+$, 526 (13) $[CuP_2]^+$, 354 (63) $[CuL]^+$. – **IR** (ATR) $\tilde{\nu}$ [cm^{-1}] = 1497 (vw), 1454 (w), 1366 (vw), 1211 (w), 1157 (w), 1121 (w), 1094 (w), 1006 (m), 904 (w), 882 (w), 805 (w), 746 (m), 630 (w), 593 (w), 494 (m), 417 (w). – **Elemental anal.** calcd for $C_{43}H_{36}Cu_2I_2NO_6P_3$ (1134.8): C 45.44, H 3.19, N 1.23; found: C 45.38, H 3.31, N 1.25. The molecular structure of the complex was determined by single crystal X-ray diffraction (CCDC 1996800).

[(2-(Bis(4-methylphenyl)phosphino)pyridin)(tris(4-fluorophenyl)phosphine)$_2$Cu$_2$I$_2$] (**Cu-1a-F**)

Complex **Cu-1a-F** was synthesized according to the general procedure and crystallized from a DCM solution layered over with *n*-pentane. The product was obtained as a pale yellow powder (88% yield).

^{1}H NMR (400 MHz, DMSO-d_6) δ [ppm] = 8.68 (bs, 1H, $H_{L(Pyr)}$), 7.89 (t, $^3J_{HH}$ = 1.8 Hz, 1H, $H_{L(Pyr)}$), 7.45 – 7.44 (m, 15H, H_P, H_L), 7.23 (t, $^3J_{HH}$ = 8.7 Hz, 15H, H_P, H_L), 7.11 (d, $^3J_{HH}$ = 7.6 Hz, 4H, $H_{L(Tolyl)}$), 2.29 (s, 6H, $H_{L(Me)}$). – **^{13}C NMR** (101 MHz, DMSO-d_6) δ [ppm] = 164.5 (s), 162.0 (s), 139.9 (s), 135.9 (dd, J = 15.1 Hz, J = 8.8 Hz), 133.4 (bs), 129.2 (bs), 128.9 (bs), 115.9 (dd, J = 20.3 Hz, J = 7.7 Hz), 21.5 (s, 2C), 20.9 (s, 2C, $C_{L(Me)}$). – **^{31}P NMR** (162 MHz, DMSO-d_6) δ [ppm] = –5.83 (bs, 1P, P_L), –11.85 (bs, 2P, P_P). – **^{19}F NMR** (376 MHz, DMSO-d_6) δ [ppm] = –114.85 (s, 6F). – **MS** (FAB, 3-NBA) m/z [%] = 1365 (5) $[M+Cu]^+$, 1176 (3) $[M–I]^+$, 1049 (9) $[Cu_3I_2LP]^+$, 1024 (19) $[Cu_3I_2L_2]^+$, 884 (20) $[Cu_2IP_2]^+$, 859 (31) $[Cu_2ILP]^+$, 733 (77) $[Cu_3I_2L]^+$, 695 (81) $[CuP_2]^+$, 670 (71) $[CuLP]^+$. – **IR** (ATR) $\tilde{\nu}$ [cm^{-1}] = 1584 (w), 1493 (m), 1453 (w), 1392 (w), 1300 (vw), 1223 (w), 1158 (w), 1093 (w), 1013 (vw), 828 (m), 809 (m), 754 (w), 708 (vw), 631 (w), 618 (vw), 517 (m), 486 (w), 470 (w), 442 (w), 431 (m), 411 (w). – **Elemental anal.** calcd for $C_{55}H_{42}Cu_2F_6I_2NP_3$ (1302.9): C 50.63, H 3.24, N 1.07; found: C 50.69, H 3.28, N 1.12. The molecular structure of the complex was determined by single crystal X-ray diffraction (CCDC 1996795).

[(2-(Bis(4-methylphenyl)phosphino)-4-methylpyridine)$_3$$Cu_2I_2$] (**Cu-1b**)

Complex **Cu-1b** was synthesized according to the general procedure and crystallized from a mixture of DCM and *n*-pentane by the layering approach. The product was obtained as a pale yellow powder (62% yield).

^{1}H NMR (400 MHz, DMSO-d_6) δ [ppm] = 8.75 (bs, 3H, $H_{L(Pyr)}$), 7.34 – 7.23 (m, 18H, $H_{L(Pyr)}$, $H_{L(Tolyl)}$), 7.08 (d, J_{CP} = 7.6 Hz, 12H, $H_{L(Tolyl)}$), 2.28 (s, 18H, $H_{L(Me)}$), 2.24 (s, 9H, $H_{L(Me)}$). – **^{13}C NMR** (101 MHz, DMSO-d_6) δ [ppm] = 158.3 (d, J_{CP} = 54.7 Hz, 3C, $C_{qL(Pyr)}$), 150.5 (d, J_{CP} = 11.2 Hz, 3C, $C_{L(Pyr)}$), 148.4 (bs, 3C, $C_{qL(Pyr)}$), 139.6 (s, 6C, $C_{qL(Tolyl)}$), 133.5 (d, J_{CP} = 12.8 Hz, 12C, $C_{L(Tolyl)}$), 131.6 – 131.3 (m, 3C, $C_{L(Pyr)}$), 129.0 (d, J_{CP} = 5.8 Hz, 12C, $C_{L(Tolyl)}$), 128 (bs, 6C, $C_{qL(Tolyl)}$), 125.6 (bs, 3C, $C_{L(Pyr)}$), 20.9 (s, 6C, $C_{L(Me)}$), 20.6 (s, 3C, $C_{L(Me)}$). – **^{31}P NMR** (162 MHz, DMSO-d_6) δ [ppm] = –7.08 (bs, 3P). – **MS** (FAB, 3-NBA) m/z [%] = 1357 (1) $[M+Cu]^+$, 1052 (11) $[Cu_3I_2L_2]^+$, 863 (8) $[Cu_2IL_2]^+$, 747 (18) $[Cu_3I_2L]^+$, 673 (32) $[CuL_2]^+$, 557 (45) $[Cu_2IL]^+$, 368 (100) $[CuL]^+$, 306 (9) $[L+H]^+$, 213 (12) $[P(Tolyl)_2]^+$. – **IR** (ATR) $\tilde{\nu}$ [cm^{-1}] = 2916 (vw), 2077 (vw), 1591 (vw), 1547 (vw), 1497 (vw), 1444 (vw), 1396 (vw), 1310 (vw), 1188 (vw), 1095 (vw), 1019 (vw), 988 (vw), 802 (vw), 740 (vw), 708 (vw), 631 (vw), 619 (vw), 554 (vw), 505 (w), 440 (vw), 409 (vw). – **Elemental anal.** calcd for $C_{60}H_{60}Cu_2I_2N_3P_3$ (1295.0): C 55.56, H 4.66, N 3.24; found: C 51.05, H 4.22, N 2.95. Reproduction of the reaction gave identical values for the elemental analysis. The molecular structure of complex **Cu-1b** was confirmed *via* single X-ray diffraction analysis (CCDC 1996738).

[(2-(Bis(4-methylphenyl)phosphino)-4-methylpyridine)-(triphenylphosphine)$_2$$Cu_2I_2$] (**Cu-1b-H**)

Complex **Cu-1b-H** was synthesized according to the general procedure and crystallized with the layering method from DCM and *n*-pentane. The product was obtained as a pale yellow powder (99% yield).

^{1}H NMR (400 MHz, DMSO-d_6) δ [ppm] = 7.46 – 7.35 (m, 33H, H_P, $H_{L(Pyr)}$), 7.18 (bs, 4H, $H_{L(Tolyl)}$), 7.08 (d, $^3J_{HH}$ = 7.7 Hz, 4H, $H_{L(Tolyl)}$), 2.28 (s, 6H, $H_{L(Me)}$), 2.23 (s, 3H, $H_{L(Me)}$). – **^{13}C NMR** (101 MHz, DMSO-d_6) δ [ppm] = 139.7 (s), 133.6 (d, J_{CP} = 13.9 Hz), 132.9 (d, J_{CP} = 28.2 Hz), 129.9 (s), 129.2 (d, J_{CP} = 8.3 Hz), 128.6 (d, J_{CP} = 8.2 Hz), 20.9 (s, 2C, $C_{L(Me)}$), 20.7 (s, 1C, $C_{L(Me)}$). – **^{31}P NMR** (162 MHz, DMSO-d_6) δ [ppm] = –5.50 (bs, 1P, P_L), –7.47 (bs, 2P, P_P). – **MS** (FAB, 3-NBA) m/z [%] = 1271 (3) $[M+Cu]^+$, 1242 (8) $[Cu_4I_3L_2]^+$, 1082 (2) $[M–I]^+$, 1052 (20) $[Cu_3I_2L_2]^+$, 1009 (4) $[Cu_3I_2LP]^+$, 966 (2) $[Cu_3I_2P_2]^+$, 819 (16) $[Cu_2ILP]^+$, 776 (12) $[Cu_2IP_2]^+$, 747 (49) $[Cu_3I_2L]^+$, 673 (68) $[CuL_2]^+$, 630 (73) $[CuLP]^+$, 587 (85) $[CuP_2]^+$, 557 (100) $[Cu_2IL]^+$. – **IR** (ATR) $\tilde{\nu}$ [cm^{-1}] = 3048 (vw), 1596 (vw), 1479 (w), 1434 (w), 1187 (vw), 1093 (w), 1029 (vw), 1000 (vw), 806 (w), 745 (w), 694 (m), 618 (vw), 515 (m), 502 (m), 463 (w), 439 (w). – **Elemental anal.** calcd for $C_{56}H_{50}Cu_2I_2NP_3$ (1208.9): C 55.55, H 4.16, N 1.16; found: C 54.97, H 4.07, N 1.16. The molecular structure of the complex was determined by single crystal X-ray diffraction (CCDC 1996792).

[(2-(Bis(4-methylphenyl)phosphino)-4-methylpyridin)(tris(4-methoxyphenyl)phosphine)$_2$$Cu_2I_2$] (**Cu-1b-MeO**)

Complex **Cu-1b-MeO** was synthesized according to the general procedure and crystallized from DCM and *n*-pentane. The product was obtained as a pale yellow powder (98% yield).

^{1}H NMR (400 MHz, DMSO-d_6) δ [ppm] = 8.55 (bs, 1H, $H_{L(Pyr)}$), 7.38 – 7.34 (m, 14H, H_P, $H_{L(Pyr)}$), 7.22 (bs, 4H, $H_{L(Tolyl)}$), 7.08 (d, $^3J_{HH}$ = 7.8 Hz, 4H, $H_{L(Tolyl)}$), 6.89 (d, $^3J_{HH}$ = 8.1 Hz, 12H, H_P), 3.75 (s, 18H, $H_{P(MeO)}$), 2.29 (s, 6H, $H_{L(Me)}$), 2.27 (s, 3H, $H_{L(Me)}$). – **^{13}C NMR** (101 MHz, DMSO-d_6) δ [ppm] = 160.3 (s), 150.8 (bs), 149.3 (bs), 139.6 (s), 135.1 (d, J_{CP} = 15.0 Hz), 133.4 (d, J_{CP} = 13.7 Hz), 132.0 (bs), 129.2 (d, J_{CP} = 7.9 Hz), 125.9 (bs), 124.7 (d, J_{CP} = 33.1 Hz), 114.1 (d, J_{CP} = 9.3 Hz), 55.1 (s, 6C, $C_{P(MeO)}$), 20.9 (s, 2C, $C_{L(Me)}$), 20.6 (s, 1C, $C_{L(Me)}$). – **^{31}P NMR** (162 MHz, DMSO-d_6) δ [ppm] = –5.91 (bs, 1P, P_L), –13.29 (bs, 2P, P_P). – **MS** (FAB, 3-NBA) m/z [%] = 1451 (3) $[M+Cu]^+$, 1262 (2) $[M–I]^+$, 1099 (6) $[Cu_3I_2LP]^+$, 1052 (17) $[Cu_3I_2L_2]^+$, 910 (25) $[Cu_2ILP]^+$, 747 (42) $[Cu_3I_2L]^+$, 720 (100) $[CuLP]^+$, 557 (66) $[Cu_2IL]^+$, 415 (16) $[CuP]^+$, 368 (81) $[CuL]^+$, 353 (20) $[P+H]^+$, 306 (10) $[L+H]^+$. – **IR** (ATR) $\tilde{\nu}$ [cm^{-1}] = 2834 (vw), 1592 (w), 1568 (w), 1497 (m), 1459 (w), 1402 (vw), 1285 (w), 1247 (m), 1177 (m), 1097 (m), 1026 (m), 824 (w), 797 (m), 717 (vw), 617 (vw), 532 (w), 505 (w), 454 (w), 417 (w). – **Elemental anal.** calcd for $C_{62}H_{62}Cu_2I_2NO_6P_3$ (1389.0): C 53.54, H 4.49, N 1.01; found: C 51.23, H 4.26, N 0.98. The molecular structure of the complex was determined by single crystal X-ray diffraction (CCDC 1996798).

[(2-(Bis(4-methylphenyl)phosphino)-4-methylpyridin)(tris(4-fluorophenyl)phosphine)$_2$$Cu_2I_2$] (**Cu-1b-F**)

Complex **Cu-1b-F** was synthesized according to the general procedure and crystallized from DCM and *n*-pentane. The product was obtained as a pale yellow powder (94% yield).

^{1}H NMR (400 MHz, DMSO-d_6) δ [ppm] = 8.42 (bs, 1H, $H_{L(Pyr)}$), 7.47 – 7.46 (m, 13H, H_P, $H_{L(Pyr)}$), 7.24 – 7.20 (m, 17H, H_P, $H_{L(Pyr)}$, $H_{L(Tolyl)}$), 7.10 (d, $^3J_{HH}$ = 7.6 Hz, 4H, $H_{L(Tolyl)}$), 2.30 (s, 6H, $H_{L(Me)}$), 2.26 (s, 3H, $H_{L(Me)}$). – **^{13}C NMR** (101 MHz, DMSO-d_6) δ [ppm] = 164.4 (s), 162.0 (s), 139.8 (s), 136.0 (dd, J = 15.6 Hz, J = 8.5 Hz), 133.4 (d, J = 14.6 Hz), 129.2 (d, J = 7.2 Hz), 128.9 (bs), 115.9 (dd, J = 21.1 Hz, J = 9.0 Hz), 20.9 (s, 2C, $C_{L(Me)}$), 20.6 (s, 1C, $C_{L(Me)}$). – **^{31}P NMR** (162 MHz, DMSO-d_6) δ [ppm] = –5.60 (bs, 1P, P_L), –13.76 (bs, 2P, P_P). – **^{19}F NMR** (376 MHz, DMSO-d_6) δ [ppm] = –114.90 (s, 6F). – **MS** (FAB, 3-NBA) m/z [%] = 1379 (2) $[M+Cu]^+$, 1190 (1) $[M–I]^+$, 1063 (1) $[Cu_3I_2LP]^+$, 873 (4) $[Cu_2ILP]^+$, 747 (7) $[Cu_3I_2L]^+$, 684 (8) $[CuLP]^+$, 557 (19) $[Cu_2IL]^+$, 378 (8) $[CuP]^+$, 368 (27) $[CuL]^+$. – **IR** (ATR) $\tilde{\nu}$ [cm^{-1}] = 2954 (vw), 1585 (m), 1494 (m), 1463 (w), 1393 (w), 1300 (vw), 1231 (m), 1159 (m), 1093 (m), 1013 (w), 826 (m), 740 (w), 708 (w), 632 (w), 618 (w), 516 (s), 503 (m), 468 (w), 457 (w), 431 (m). – **Elemental anal.** calcd for $C_{56}H_{44}Cu_2F_6I_2NP_3$ (1316.9): C 51.00, H 3.36, N 1.06; found: C 51.13, H 3.55, N 1.06. The molecular structure of the complex was determined by single crystal X-ray diffraction (CCDC 1996797).

[(2-(Bis(4-methoxyphenyl)phosphino)pyridine)(triphenylphosphine)$_2$Cu$_2$I$_2$] (**Cu-2a-H**)

Complex **Cu-2a-H** was synthesized according to the general procedure and crystallized with the layering method from DCM and *n*-pentane. The product was obtained as a pale yellow powder (73% yield).

^{1}H NMR (400 MHz, DMSO-d_6) δ [ppm] = 8.61 (bs, 1H, $H_{L(Pyr)}$), 7.86 (t, $^3J_{HH}$ = 7.5 Hz, 1H, $H_{L(Pyr)}$), 7.57 (d, $^3J_{HH}$ = 7.4 Hz, 1H, $H_{L(Pyr)}$), 7.45 – 7.42 (m, 19H, H_P, $H_{L(Pyr)}$), 7.36 – 7.32 (m, 16H, H_P, $H_{L(MeO\text{-}Ph)}$), 6.84 (d, $^3J_{HH}$ = 8.4 Hz, 4H, $H_{L(MeO\text{-}Ph)}$), 3.75 (s, 6H, $H_{L(MeO)}$). – **^{13}C NMR** (101 MHz, DMSO-d_6) δ [ppm] = 160.5 (s), 151.0 (bs), 137.6 (bs), 135.3 (d, J_{CP} = 13.2 Hz), 133.7 (d, J_{CP} = 13.5 Hz), 133.2 (d, J_{CP} = 27.4 Hz), 129.8 (s), 128.5 (d, J_{CP} = 8.3 Hz), 124.6 (bs), 123.1 (d, J_{CP} = 25.3 Hz), 114.2 (d, J_{CP} = 5.2 Hz), 55.2 (s, 2C, $C_{L(MeO)}$). – **^{31}P NMR** (162 MHz, DMSO-d_6) δ [ppm] = –7.31 (bs, 1P, P_L), –9.94 (bs, 2P, P_P). – **MS** (FAB, 3-NBA) m/z [%] = 1289 (2) $[M+Cu]^+$, 1227 (1) $[M+H]^+$, 1100 (3) $[M–I]^+$, 1027 (2) $[Cu_3I_2LP]^+$, 837 (6) $[Cu_2ILP]^+$, 648 (11) $[CuLP]^+$, 587 (23) $[CuP_2]^+$, 575 (12) $[Cu_2IL]^+$, 386 (16) $[CuL]^+$. – **IR** (ATR) $\tilde{\nu}$ [cm^{-1}] = 3048 (vw), 1593 (w), 1498 (w), 1479 (w), 1452 (vw), 1433 (w), 1287 (w), 1250 (w), 1178 (w), 1094 (w), 1026 (w), 825 (w), 798 (vw), 743 (w), 693 (m), 518 (w), 506 (w), 426 (vw). – **Elemental anal.** calcd for $C_{55}H_{48}Cu_2I_2NO_2P_3$ (1226.8): C 53.76, H 3.94, N 1.14; found: C 53.43, H 3.92, N 1.19. The molecular structure of the complex was determined by single crystal X-ray diffraction (CCDC 1996799).

[(2-(Bis(4-methoxyphenyl)phosphino)-4-metylpyridine)-(triphenylphosphine)$_2$Cu$_2$I$_2$] (**Cu-2b-H**)

Complex **Cu-2b-H** was synthesized according to the general procedure and crystallized with the layering method from DCM and *n*-pentane. The product was obtained as a pale yellow powder (60% yield).

^{1}H NMR (400 MHz, DMSO-d_6) δ [ppm] = 8.44 (bs, 1H, $H_{L(Pyr)}$), 7.43 (t, $^3J_{HH}$ = 7.4 Hz, 19H, H_P, $H_{L(Pyr)}$), 7.34 (t, $^3J_{HH}$ = 7.1 Hz, 12H, H_P), 7.29 (bs, 4H, $H_{L(Tolyl)}$), 7.21 (bs, 1H, $H_{L(Pyr)}$), 6.82 (d, $^3J_{HH}$ = 36.6 Hz, 4H, $H_{L(Tolyl)}$), 3.75 (s, 6H, $H_{L(MeO)}$), 2.25 (s, 3H, $H_{L(Me)}$). – **^{13}C NMR** (101 MHz, DMSO-d_6) δ [ppm] = 169.6 (s), 160.5 (s), 150.6 (bs), 135.2 (d, J_{CP} = 11.9 Hz), 133.7 (d, J_{CP} = 13.7 Hz), 133.2 (d, J_{CP} = 27.4 Hz), 131.6 (bs), 129.8 (s), 128.5 (d, J_{CP} = 8.0 Hz), 125.6 (bs), 123.1 (bs), 114.1 (d, J_{CP} = 7.3 Hz), 55.2 (s, 2C, $C_{L(MeO)}$), 20.6 (s, 1C, $C_{L(Me)}$). – **^{31}P NMR** (162 MHz, DMSO-d_6) δ [ppm] = –6.90 (bs, 1P, P_L), –10.80 (bs, 2P, P_P). – **MS** (FAB, 3-NBA) m/z [%] = 1303 (5) $[M+Cu]^+$, 1241 (3) $[M+H]^+$, 1114 (15) $[M–I]^+$, 1041 (10) $[Cu_3I_2LP]^+$, 966 (1) $[Cu_3I_2P_2]^+$, 927 (11) $[Cu_2IL_2]^+$, 851 (84) $[Cu_2ILP]^+$, 779 (84) $[Cu_3I_2L]^+$, 776 (63) $[Cu_2IP_2]^+$, 737 (30) $[CuL_2]^+$. – **IR** (ATR) $\tilde{\nu}$ [cm^{-1}] = 3048 (vw), 1593 (w), 1498 (m), 1478 (w), 1433 (m), 1287 (w), 1250 (m), 1177 (m), 1093 (m), 1025 (w), 824 (w), 798 (w), 743 (m), 693 (m), 516 (m), 502 (m), 469 (w), 444 (w), 387 (vw). – **Elemental anal.** calcd for $C_{56}H_{50}Cu_2I_2NO_2P_3$ (1240.9): C 54.12, H 4.06, N 1.13; found: C 53.83, H 4.00, N 1.17. The molecular structure of the complex was determined by single crystal X-ray diffraction (CCDC 1996801).

[(2-(Bis(3,5-dimethylphenyl)phosphino)pyridine)(triphenylphosphine)$_2$Cu$_2$I$_2$] (**Cu-3a-H**)

Complex **Cu-3a-H** was synthesized according to the general procedure. For precipitation the resulting solution was directly poured into *n*-pentane. The complex was crystallized from DCM and *n*-pentane. The product was obtained as a pale yellow powder (33% yield).

^{1}H NMR (400 MHz, DMSO-d_6) δ [ppm] = 8.61 (bs, 1H, $H_{L(Pyr)}$), 7.81 (bs, 1H, $H_{L(Pyr)}$), 7.49 (bs, 1H, $H_{L(Pyr)}$), 7.43 – 7.37 (m, 19H, H_P, $H_{L(Pyr)}$), 7.31 (t, $^3J_{HH}$ = 7.4 Hz, 12H, H_P), 7.01 (bs, 6H, H_L), (s, 12H, $H_{L(Me)}$). – **^{13}C NMR** (101 MHz, DMSO-d_6) δ [ppm] = 150.7 (bs), 137.4 (d, J_{CP} = 6.3 Hz), 133.6 (d, J_{CP} = 13.8 Hz), 133.2 (d, J_{CP} = 26.2 Hz), 131.5 (s), 131.3 (bs), 129.8 (s), 128.4 (d, J_{CP} = 8.2 Hz). – **^{31}P NMR** (162 MHz, DMSO-d_6) δ [ppm] = –5.26 (bs, 1P, P_L), –8.48 (bs, 2P, P_P). – **MS** (FAB, 3-NBA) m/z [%] = 1080 (4) $[Cu_3I_2L_2]^+$, 1023 (2) $[Cu_3I_2LP]^+$, 834 (9) $[Cu_2ILP]^+$, 761 (19) $[Cu_3I_2L]^+$, 704 (8) $[Cu_3I_2P]^+$, 644 (40) $[CuLP]^+$, 587 (39) $[CuP_2]^+$, 571 (36) $[Cu_2IL]^+$, 514 (13) $[Cu_2IP]^+$, 382 (100) $[CuL]^+$, 325 (46) $[CuP]^+$, 320 (13) $[L+H]^+$, 263 (23) $[P+H]^+$, 185 (9) $[PPh_2]^+$. – **IR** (ATR) $\tilde{\nu}$ [cm^{-1}] = 3049 (vw), 1583 (vw), 1479 (vw), 1434 (w), 1183 (vw), 1157 (vw), 1127 (vw), 1094 (w), 1027 (vw), 998 (vw), 846 (vw), 742 (w), 692 (m), 618 (vw), 563 (vw), 519 (w), 505 (w), 431 (vw). – **Elemental anal.** calcd for $C_{57}H_{52}Cu_2I_2NP_3$ (1222.9): C 55.89, H 4.28, N 1.14; found: C 53.84, H 4.01, N 0.88. The molecular structure of the complex was determined by single crystal X-ray diffraction (CCDC 1996739).

[(4-Methyl-2-(bis(3,5-dimethylphenyl)phosphino)pyridine)(triphenylphosphine)$_2$Cu$_2$I$_2$] (**Cu-3b-H**)

Complex **Cu-3b-H** was synthesized according to the general procedure. The product was obtained as a pale yellow powder (77% yield).

^{1}H NMR (400 MHz, DMSO-d_6) δ [ppm] = 7.45 – 7.32 (m, 37H, H_P, H_L), 7.00 (bs, 2H, H_L), 2.28 (bs, 3H, $H_{L(Me)}$), 2.08 (bs, 12H, $H_{L(Me)}$). – **^{13}C NMR** (101 MHz, DMSO-d_6) δ [ppm] = 137.5 (d, J_{CP} = 6.5 Hz), 133.6 (d, J_{CP} = 14.0 Hz), 133.0 (d, J_{CP} = 28.5 Hz), 131.5 (s), 131.0 (bs), 129.9 (s), 128.5 (d, J_{CP} = 8.2 Hz), 20.9 (s, 4C, $C_{L(Me)}$), 20.6 (s, 1C, $C_{L(Me)}$). – **^{31}P NMR** (162 MHz, DMSO-d_6) δ [ppm] = –4.99 (bs, 1P, P_L), –8.27 (bs, 2P, P_P). – **MS** (FAB, 3-NBA) *m/z* [%] = 1299 (7) $[M+Cu]^+$, 1110 (17) $[M–I]^+$, 1037 (5) $[Cu_3I_2LP]^+$, 848 (20) $[Cu_2ILP]^+$, 775 (36) $[Cu_3I_2L]^+$, 658 (67) $[CuLP]^+$, 585 (70) $[Cu_2IL]^+$, 396 (100) $[CuL]^+$, 325 (32) $[CuP]^+$, 263 (21) $[P+H]^+$. – **IR** (ATR) $\tilde{\nu}$ [cm^{-1}] = 3050 (vw), 1586 (vw), 1479 (vw), 1434 (w), 1183 (vw), 1126 (vw), 1094 (w), 1027 (vw), 997 (vw), 846 (vw), 742 (w), 691 (w), 661 (vw), 519 (w), 444 (w). – **Elemental anal.** calcd for $C_{58}H_{54}Cu_2I_2NP_3$ (1237.0): C 56.23, H 4.39, N 1.13; found: C 54.81, H 4.19, N 0.99.

[(4-Methyl-2-(bis(3,5-dimethylphenyl)phosphino)pyridine)(tris(4-fluorophenyl)phosphine)$_2$Cu$_2$I$_2$] (**Cu-3b-F**)

Complex **Cu-3b-F** was synthesized according to the general procedure and crystallized with the layering method from DCM and *n*-pentane. The product was obtained as a pale yellow powder (95% yield).

^{1}H NMR (400 MHz, DMSO-d_6) δ [ppm] = 8.38 (bs, 1H, $H_{L(Pyr)}$), 7.77 – 7.63 (m, 1H, $H_{L(Pyr)}$), 7.49 (bs, 13H, $H_{L(Pyr)}$, H_P), 7.20 (bs, 12H, H_P), 7.02 (bs, 6H, H_L), 2.27 (s, 3H, $H_{L(Me)}$), 2.09 (s, 12H, $H_{L(Me)}$). – **^{13}C NMR** (101 MHz, DMSO-d_6) δ [ppm] = 164.4 (s, C_q), 161.9 (s, C_q), 150.7 (d, *J* = 14.1 Hz), 149.5 (bs, C_q), 137.5 (d, *J* = 8.1 Hz), 136.0 (dd, *J* = 15.6 Hz, *J* = 8.4 Hz), 134.4 (dd, *J* = 11.5 Hz, *J* = 9.0 Hz), 131.5 (s), 131.0 (d, *J* = 13.4 Hz), 129.1 (dd, *J* = 28.8 Hz, *J* = 3.3 Hz, C_q), 126.1 (bs), 115.8 (dd, *J* = 21.3 Hz, *J* = 9.3 Hz), 20.8 (s, 4C, $C_{L(Me)}$), 20.5 (s, 1C, $C_{L(Me)}$). – **^{31}P NMR** (162 MHz, DMSO-d_6) δ [ppm] = –4.93 (bs, 1P, P_L), –15.06 (bs, 2P, P_P). – **^{19}F NMR** (376 MHz, DMSO-d_6) δ [ppm] = –114.92 (s, 6F). – **MS** (FAB, 3-NBA) *m/z* [%] = 1407 (1) $[M+Cu]^+$, 1298 (2) $[Cu_4I_3L_2]^+$, 1108 (5) $[Cu_3I_2L_2]^+$, 901 (8) $[Cu_2ILP]^+$, 775 (39) $[Cu_3I_2L]^+$, 695 (6) $[CuP_2]^+$, 585 (68) $[Cu_2IL]^+$, 568 (5) $[Cu_2IP]^+$, 396 (100) $[CuL]^+$, 378 (16) $[CuP]^+$, 317 (13) $[P+H]^+$, 227 (9) $[L–Pyr–Me]^+$. – **IR** (ATR) $\tilde{\nu}$ [cm^{-1}] = 2917 (vw), 1895 (vw), 1586 (m), 1493 (m), 1393 (w), 1301 (vw), 1224 (m), 1158 (m), 1092 (w), 1039 (w), 1013 (w), 823 (m), 740 (vw), 709 (w), 689 (w), 634 (vw), 610 (vw), 562 (vw), 522 (m), 466 (w), 442 (m). – **Elemental anal.** calcd for $C_{58}H_{48}Cu_2F_6I_2NP_3$ (1346.9): C 51.72, H 3.59, N 1.04; found: C 51.27, H 3.54, N 1.13.

[(2-(Bis(2-furyl)phosphino)pyridine)(triphenylphosphine)$_2$Cu$_2$I$_2$] (**Cu-5a-H**)

Complex **Cu-5a-H** was synthesized according to the general procedure and crystallized with the layering method from DCM and *n*-pentane. The product was obtained as a pale yellow powder (95% yield).

^{1}H NMR (400 MHz, DMSO-d_6) δ [ppm] = 8.58 (bs, 1H, $H_{L(Pyr)}$), 7.97 (d, $^3J_{HH}$ = 0.8 Hz, 2H, $H_{L(Furyl)}$), 7.92 (t, $^3J_{HH}$ = 7.1 Hz, 1H, $H_{L(Pyr)}$), 7.64 (bs, 1H, $H_{L(Pyr)}$), 7.51 – 7.35 (m, 32H, H_P, $H_{L(Furyl)}$), 6.88 (bs, 1H, $H_{L(Pyr)}$), 6.50 (s, 2H, $H_{L(Furyl)}$). – **^{13}C NMR** (101 MHz, DMSO-d_6) δ [ppm] = 156.5 (d, J_{CP} = 55.2 Hz), 150.9 (bs), 149.2 (d, J_{CP} = 1.4 Hz), 144.7 (d, J_{CP} = 32.6 Hz), 137.7 (bs), 133.7 (d, J_{CP} = 14.0 Hz), 133.0 (d, J_{CP} = 28.7 Hz), 129.9 (s), 128.5 (d, J_{CP} = 8.7 Hz), 125.0 (bs), 124.4 (d, J_{CP} = 18.9 Hz), 111.1 (d, J_{CP} = 7.6 Hz). – **^{31}P NMR** (162 MHz, DMSO-d_6) δ [ppm] = –9.81 (bs, 2P, P_P),–47.56 (bs, 1P, P_L). – **MS** (FAB, 3-NBA) *m/z* [%] = 1209 (11) $[M+Cu]^+$, 1147 (3) $[M+H]^+$, 1019 (20) $[M–I]^+$, 966 (6) $[Cu_3I_2P_2]^+$, 947 (11) $[Cu_3I_2LP]^+$, 928 (25) $[Cu_3I_2L_2]^+$, 776 (100) $[Cu_2IP_2]^+$, 757 (66) $[Cu_2ILP]^+$, 704 (12) $[Cu_3I_2P_2]^+$, 685 (53) $[Cu_3I_2L]^+$. – **IR** (ATR) $\tilde{\nu}$ [cm^{-1}] = 3046 (vw), 1580 (vw), 1478 (w), 1452 (vw), 1433 (w), 1211 (vw), 1155 (w), 1115 (w), 1093 (w), 1027 (vw), 1007 (w), 903 (w), 882 (vw), 742 (m), 692 (m), 593 (w), 518 (m), 505 (m), 466 (w). – **Elemental anal.** calcd for $C_{49}H_{40}Cu_2I_2NO_2P_3$ (1146.8): C 51.24, H 3.51, N 1.22; found: C 50.60, H 3.51, N 1.12. The molecular structure of the complex was determined by single crystal X-ray diffraction (CCDC 1996793).

[(2-(Bis(2-furyl)phosphino)pyridine)(tris(4-fluorophenyl)phosphine)$_2$Cu$_2$I$_2$] (**Cu-5a-F**)

Complex **Cu-5a-F** was synthesized according to the general procedure and crystallized with the layering method from DCM and *n*-pentane. The product was obtained as a pale yellow powder (92% yield).

^{1}H NMR (400 MHz, DMSO-d_6) δ [ppm] = 8.57 (bs, 1H, $H_{L(Pyr)}$), 7.99 (bs, 2H, $H_{L(Furyl)}$), 7.95 (t, $^3J_{HH}$ = 7.7 Hz, 1H, $H_{L(Pyr)}$), 7.65 (bs, 1H, $H_{L(Pyr)}$), 7.54 – 7.44 (m, 14H, H_L, H_P), 7.25 (t, $^3J_{HH}$ = 8.8 Hz, 12H, H_P), 6.88 (bs, 1H, $H_{L(Pyr)}$), 6.53 (bs, 2H, $H_{L(Furyl)}$). – **^{13}C NMR** (101 MHz, DMSO-d_6) δ [ppm] = 164.5 (s), 162.0 (s), 156.6 (bs), 156.1 (bs), 151.0 (bs), 149.3 (d, *J* = 2.1 Hz), 144.5 (d, *J* = 34.9 Hz), 137.9 (bs), 136.0 (dd, *J* = 15.6 Hz, *J* = 8.5 Hz), 128.9 (dd, *J* = 29.3 Hz, *J* = 2.8 Hz), 125.3 (bs), 124.2 (d, *J* = 23.1 Hz), 115.9 (dd, *J* = 21.2 Hz, *J* = 9.6 Hz), 111.2 (d, *J* = 7.3 Hz). – **^{31}P NMR** (162 MHz, DMSO-d_6) δ [ppm] = –13.35 (bs, 2P, P_P), –46.39 (bs, 1P, P_L). – **^{19}F NMR** (376 MHz, DMSO-d_6) δ [ppm] = –110.39 (s, 6F). – **MS** (FAB, 3-NBA) *m/z* [%] = 1317 (5) $[M+Cu]^+$, 1255 (3) $[M+H]^+$, 1227 (10) $[M–I]^+$, 1074 (16) $[Cu_3I_2P_2]^+$, 1001 (14) $[Cu_3I_2LP]^+$, 928 (25) $[Cu_3I_2L_2]^+$, 884 (100) $[Cu_2IP_2]^+$, 811 (67) $[Cu_2ILP]^+$. – **IR** (ATR) $\tilde{\nu}$ [cm^{-1}] = 1584 (w), 1493 (m), 1393 (w), 1300 (vw), 1221 (m), 1159 (m), 1124 (w), 1093 (w), 1007 (w), 903 (vw), 825 (m), 812 (m), 860 (w), 748 (m), 635 (w), 590 (vw), 516 (m), 461 (m), 433 (m), 407 (w). – **Elemental anal.** calcd for $C_{49}H_{34}Cu_2F_6I_2NO_2P_3$ (1254.8): C 46.83, H 2.73, N 1.11; found: C 47.08, H 2.57, N 1.22. The molecular structure of the complex was determined by single crystal X-ray diffraction (CCDC 1996794).

[(2-(Bis(2-furyl)phosphino)-4-methylpyridine)(triphenylphosphine)$_2$Cu$_2$I$_2$] (**Cu-5b-H**)

Complex **Cu-5b-H** was synthesized according to the general procedure. The complex was crystallized from DCM and *n*-pentane. The product was obtained as a pale yellow powder (72% yield).

^{1}H NMR (400 MHz, DMSO-d_6) δ [ppm] = 8.45 (bs, 1H, $H_{L(Pyr)}$), 7.95 (s, 2H, $H_{L(Furyl)}$), 7.46 – 7.34 (m, 32H, H_P, $H_{L(Furyl)}$), 7.21 (bs, 1H, $H_{L(Pyr)}$), 6.98 (bs, 1H, $H_{L(Pyr)}$), 6.53 (s,

2H, $H_{L(Furyl)}$), 2.25 (s, 3H, $H_{L(Me)}$). – **^{13}C NMR** (101 MHz, DMSO-d_6) δ [ppm] = 149.0 (bs), 133.6 (d, J_{CP} = 14.2 Hz), 133.0 (d, J_{CP} = 28.0 Hz), 129.9 (s), 128.6 (d, J_{CP} = 8.1 Hz), 111.2 (d, J_{CP} = 7.7 Hz), 20.7 (s, 1C, $C_{L(Me)}$). – **^{31}P NMR** (162 MHz, DMSO-d_6) δ [ppm] = –7.65 (bs, 2P, P_P), –49.43 (bs, 1P, P_L). – **MS** (FAB, 3-NBA) *m*/*z* [%] = 1223 (1) $[M+Cu]^+$, 961 (11) $[Cu_3I_2LP]^+$. – **IR** (ATR) $\tilde{\nu}$ [cm^{-1}] = 3049 (vw), 1598 (vw), 1479 (vw), 1434 (w), 1153 (vw), 1116 (vw), 1093 (vw), 1027 (vw), 1007 (vw), 902 (vw), 882 (vw), 824 (vw), 742 (w), 693 (w), 593 (vw), 552 (vw), 510 (w), 490 (w), 458 (w), 439 (vw), 386 (vw). – **Elemental anal.** calcd for $C_{50}H_{42}Cu_2I_2NO_2P_3$ (1160.9): C 51.65, H 3.64, N 1.20; found: C 51.22, H 3.64, N 1.14. The molecular structure of the complex was determined by single crystal X-ray diffraction (CCDC 1996737).

[(2-(Bis(4-fluorophenyl)phosphino)pyridine)(triphenylphosphine)$_2$$Cu_2I_2$] (**Cu-6a-H**)

Complex **Cu-6a-H** was synthesized according to the general procedure and was crystallized from DCM and *n*-pentane. The product was obtained as a pale yellow powder (62% yield).

^{1}H NMR (400 MHz, DMSO-d_6) δ [ppm] = 8.59 (bs, 1H, $H_{L(Pyr)}$), 7.88 (t, $^3J_{HH}$ = 7.7 Hz, 1H, $H_{L(Pyr)}$), 7.66 (d, $^3J_{HH}$ = 7.8 Hz, 1H, $H_{L(Pyr)}$), 7.45 – 7.42 (m, 23H, H_P, $H_{L(Pyr)}$, $H_{L(F-Ph)}$), 7.34 (t, $^3J_{HH}$ = 7.4 Hz, 12H, H_P), 7.15 (t, $^3J_{HH}$ = 8.8 Hz, 4H, $H_{L(F-Ph)}$). – **^{13}C NMR** (101 MHz, DMSO-d_6) δ [ppm] = 164.4 (s), 162.0 (s), 151.2 (bs), 137.8 (bs), 136.1 (bs), 133.7 (d, *J* = 13.3 Hz), 133.1 (d, *J* = 27.8 Hz), 131.5 (bs), 129.9 (s), 128.5 (d, *J* = 7.5 Hz), 128.3 (bs), 125.0 (bs), 115.8 (d, *J* = 21.8 Hz). – **^{31}P NMR** (162 MHz, DMSO-d_6) δ [ppm] = –8.88 (bs, 1P, P_L), –9.88 (bs, 2P, P_P). – **^{19}F NMR** (376 MHz, DMSO-d_6) δ [ppm] = –114.72 (s, 2F). – **MS** (FAB, 3-NBA) *m*/*z* [%] = 1265 (2) $[M+Cu]^+$, 1227 (1) $[M+H]^+$, 1100 (3) $[M–I]^+$, 1027 (2) $[Cu_3I_2LP]^+$, 837 (2) $[M+Cu]^+$, 1203 (1) $[M+H]^+$, 1076 (3) $[M–I]^+$, 1003 (4) $[Cu_3I_2LP]^+$, 813 (24) $[Cu_2ILP]^+$, 776 (21) $[Cu_2IP_2]^+$, 741 (10) $[Cu_3I_2L]^+$, 624 (46) $[CuLP]^+$, 587 (62) $[CuP_2]^+$, 551 (33) $[Cu_2IL]^+$, 514 (16) $[Cu_2IP]^+$, 361 (34) $[CuL]^+$, 325 (35) $[CuP]^+$, 263 (19) $[P+H]^+$, 185 (9) $[PPh_2]^+$. – **IR** (ATR) $\tilde{\nu}$ [cm^{-1}] = 3050 (vw), 1587 (w), 1495 (w), 1480 (w), 1434 (w), 1393 (vw), 1231 (w), 1160 (w), 1092 (w), 998 (vw), 826 (w), 741 (m), 692 (m), 518 (m), 504 (m), 450 (w), 420 (w). – **Elemental anal.** calcd for $C_{53}H_{42}Cu_2F_2I_2NP_3$ (1202.9): C 52.84, H 3.51, N 1.16; found: C 52.95, H 3.53, N 1.64. The molecular structure of the complex was determined by single crystal X-ray diffraction (CCDC 1996803).

Theoretical calculations

All quantum chemical calculations in this work were performed with the Guassiano9 package using B3LYP for the geometry optimization with the basis set 6-31G(d,p) for the atoms C, H and N, and P plus the Cu and I basis set SBKJC-VDZ ECP in gas phase, with a total charge of zero. The same data settings were used for calculating the excited states *via* TDDFT. For further computational details, as well as for the other HOMO, LUMO and spin density plots, compare the corresponding section in the ESI.

OLED manufacturing

For the preparation of the OLED devices prepatterned glass substrates (1.1 mm) with indium tin oxide coatings (120 nm-160 nm, surface resistance of 15 Ohm/sq) of *Lumtec Corp.* were used as anodes (LT-G001 ITO glass). The substrates were washed sequentially in an ultrasonic bath with a NaOH solution (100 g/L NaOH in ethanol with a small portion of water, 30 min), distilled water (10 min) and 2-propanol (10 min). The component was dried under a N_2-flow afterwards. In order to remove all residuals and/or organic impurities on the surface a 30-minutes UV-treatment with the *Ossila* UV-ozone cleaner was applied. Ozone was hereby generated *via* UV-emission to oxidize and get rid of the possible residues

All prior treatments as well as the spin-coating depositions were performed under ambient air conditions in a clean-room of the class 10000.

First, a 50 nm-thick PEDOT:PSS (poly(3,4-ethylenedioxythiophene):poly(styrenesulfonate), from *Lumtec Corp.*) hole-injection layer was deposited by pouring 300 µL of the corresponding aqueous solution (2 wt%) onto the substrate, followed by rotation with 2000 rpm for 60 seconds. The obtained film was dried at 100 °C for 30 min. As next step, a 20 nm-thick hole-transporting poly-TPD (poly(4-butyltriphenylamine, from *Ossila* (UK), sublimation grade >99%) layer was spin-coated from a chlorobenzene solution (5 g/L) at 2000 rpm for 60 seconds. The layer was dried at 100 °C for 10 min. Finally, the emission layer as a mixture of the copper complex emitter material (20 wt%) in pure CBP (4,4′-bis(N-carbazolyl)-1,1′-biphenyl) or in a mixture of CBP:TcTa (7:3) with TcTa = tris(4-carbazoyl-9-ylphenyl)amine (both with a sublimation grade >99.5%) was spin-coated. In some cases also DMFL-CBP (2,7-bis-(carbazol-9-yl)-9,9-dimethylfluorene, sublimation grade >99.5%) was used as host material. Hereby dichloromethane served as solvent (5 g/L) and the rotation was performed with 1020-2120 rpm for 60 seconds respectively. For the comparison studies a standard thickness of the EML of 20 nm, which was obtained with a spin-coating frequency of 1500 rpm, was used.

After the depositions the substrates were transferred into an argon glovebox. The emission layers were dried at 80 °C for 20 min. *Via* thermal evaporation (Univex-300, *Leybord Heraeus*) a 15-30-nm-thick electron-transporting/hole-blocking layers were applied. For this layer TPBi (2,2′,2"-(1,3,5-benzinetriyl)-tris(1-phenyl-1-*H*-benzimidazol), sublimation grade >99.5%) or OXD-7 (1,3-bis[2-(4-*tert*-butylphenyl)-1,3,4-oxadiazo-5-yl]benzol, sublimation grade >99%, both from *Lumtec Corp.* (Taiwan)) were used. On top a LiF-layer (1 nm) and an aluminium layer (>100 nm) were evaporated under a pressure below 10^{-5} mbar as cathode.

The thickness of the layers was controlled by a quartz microbalance resonator pregraduated with an atomic force microscope.

Measurements of the OLED characteristics were performed in an argon glovebox as well. The electroluminescence spectra were obtained using an *Ocean Optics Maya*

2000 Pro CCD spectrometer with a sensitivity within the range of 200-1100 nm. Current intensity(I)-voltage(V) curves were recorded using two DT 838 digital multimeters. The luminance was measured by a TKA-PKM luminance meter (*TKA Instruments*).

ASSOCIATED CONTENT

Electronic Supporting Information (ESI)

The ESI material is available free of charge *via* the internet at http://pubs.acs.org.

The ESI contains further experimental and spectroscopic data as well as information about the single crystal X-ray analyses including ORTEP plots and crystallographic and refinement data. Details about the theoretical calculations (HOMO/LUMO and spin density plots), absorption spectra (DCM and neat films), photoemission yield spectroscopy (PYS) and adiabatic energy gap measurement of HOMO energies are given. Photophysical data, further details of the OLED devices, electroluminescence spectra and I-V curves are included as well. (PDF)

Data Deposition in Repositories

The details on the chemical synthesis and original analytical data were added to the repository Chemotion (www.chemotion.net/home). The crystal structures can be found on https://www.ccdc.cam.ac.uk/structures/. The corresponding codes are given in brackets. **1a** (CRR-8730), **1b** (CRR-8882), **2a** (CRR-8894), **2b** (CRR-8906, CCDC 1996735), **3a** (CRR-8919), **3b** (CRR-8930), **4a** (CRR-8941), **4b** (CRR-8988), **5a** (CRR-8992), **5b** (CRR-9003), **6a** (CRR-9119, CCDC 1996736), **Cu-1a** (CRR-9015), **Cu-1b** (CRR-11482 ,CCDC 1996738), **Cu-1a-H** (CRR-9038, CCDC 1996791), **Cu-1b-H** (CRR-9063, CCDC 1996792), **Cu-1a-MeO** (CRR-9046, CCDC 1996796), **Cu-1b-MeO** (CRR-9085, CCDC 1996798), **Cu-1a-Furyl** (CRR-9030, CCDC 1996800), **Cu-1a-F** (CRR-9021, CCDC 1996795), **Cu-1b-F** (CRR-9054, CCDC 1996797), **Cu-2a-H** (CRR-9095, CCDC 1996799), **Cu-2b-H** (CRR-9103, CCDC 1996801), **Cu-3a-H** (CRR-9111, CCDC 1996739), **Cu-3b-H** (CRR-9364, CCDC 2027314), **Cu-3b-F** (CRR-14647, CCDC 2027315), **Cu-3b-F-4** (CCDC 1996802), **Cu-5a-H** (CRR-9371, CCDC 1996793), **Cu-5b-H** (CRR-9388, CCDC 1996737), **Cu-5a-F** (CRR-9379, CCDC 1996794), and **Cu-6a-H** (CRR-9396, CCDC 1996803).

AUTHOR INFORMATION

Corresponding Authors

* Stefan Bräse: braese@kit.edu.
* Valentina V. Utochnikova: valentina.utochnikova@gmail.com.

ORCID

Jasmin M. Busch: 0000-0002-8020-8893
Daniil S. Koshelev: 0000-0001-8210-6690
Andrey A. Vashchenko: 0000-0003-2084-5900
Olaf Fuhr: 0000-0003-3516-2440
Martin Nieger: 0000-0003-1677-0109
Valentina V. Utochnikova: 0000-0002-0830-1268
Stefan Bräse: 0000-0003-4845-3191

Notes

There are no conflicts to declare.

ACKNOWLEDGMENT

This interdisciplinary project was supported by the Karlsruhe Institute of Technology (KIT) as well as by the project T1 (SFB/TRR 88 „*Cooperative Effects in Homo- and Hetero-Metallic Complexes (3MET)*“) by the Deutsche Forschungsgemeinschaft (DFG) in cooperation with the cynora GmbH. Especially we wish to thank Daniel Zink for his support. Furthermore, we would like to thank the Karlsruhe School of Optics and Photonics (KSOP) for its financial support. In addition we acknowledge the Karlsruhe House of Young Scientists (KHYS) for the Internship Grant of Daniil Koshelev. We acknowledge the financial support of MK-2799.2019.3 and RFBR 18-33-20210. We also wish to thank the Eli Zysman-Colman group for their compute power for the quantum chemical calculations. Furthermore we thank the Karlsruhe House of Young Scientists for financial support *via* the KHYS Travel Grant during the research stay of Jasmin M. Busch at the University of St. Andrews. Finally, we wish to thank the whole analytics team of the KIT.

ABBREVIATIONS

TADF, thermally activated delayed fluorescence; OLED, organic light-emitting diode; UV, ultraviolet; ITO, indium tin oxide; PEDOT, poly(3,4-ethylenedioxythiophene); PSS, poly(styrenesulfonate); poly-TPD, poly(4-butyltriphenylamine; CBP, 4,4′-bis(N-carbazolyl)-1,1′-biphenyl; TcTa, tris(4-carbazoyl-9-ylphenyl)amine; DMFL-CBP, 2,7-bis(carbazol-9-yl)-9,9-dimethylfluorene; TPBi, 2,2′,2"-(1,3,5-benzinetriyl)-tris(1-phenyl-1-*H*-benzimidazol); OXD-7, 1,3-bis[2-(4-*tert*-butylphenyl)-1,3,4-oxadiazo-5-yl]benzol; TAZ, 3-(biphenyl-4-yl)-5-(4-*tert*-butylphenyl)-4-phenyl-4H-1,2,4-triazole; rpm, revolutions per minute; CCD, Charge Coupled Device; KIT, Karlsruhe Institute of Technology; DFG, Deutsche Forschungsgemeinschaft; KSOP, Karlsruhe School of Optics and Photonics; KHYS, Karlsruhe House of Young Scientists.

REFERENCES

1. Gupta, A. K.; Kishore, P. V. V. N.; Liao, J.-H.; Chen, Y.-J.; Liu, C. W., Hexadecanuclear Copper Monothiocarbonates: An Emissive Cluster Building Block. *Eur. J. Inorg. Chem.* **2017**, 1989-1993.
2. El Moll, H.; Cordier, M.; Nocton, G.; Massuyeau, F.; Latouche, C.; Martineau-Corcos, C.; Perruchas, S., A Heptanuclear Copper Iodide Nanocluster. *Inorg. Chem.* **2018,** 57, 11961-11969.
3. Wang, J. J.; Chen, C.; Chen, W. G.; Yao, J. S.; Yang, J. N.; Wang, K. H.; Yin, Y. C.; Yao, M. M.; Feng, L. Z.; Ma, C.; Fan, F. J.; Yao, H. B., Highly Luminescent Copper Iodide Cluster Based Inks with Photoluminescence Quantum Efficiency Exceeding 98. *J. Am. Chem. Soc.* **2020,** 142, 3686-3690.
4. Zink, D. M.; Grab, T.; Baumann, T.; Nieger, M.; Barnes, E. C.; Klopper, W.; Bräse, S., Experimental and Theoretical Study of

Novel Luminescent Di-, Tri-, and Tetranuclear Copper Triazole Complexes. *Organometallics* **2011,** 30, 3275-3283.
5. Roesch, P.; Nitsch, J.; Lutz, M.; Wiecko, J.; Steffen, A.; Muller, C., Synthesis and Photoluminescence Properties of an Unprecedented Phosphinine−Cu4Br4 Cluster. *Inorg. Chem.* **2014,** 53, 9855-9859.
6. Chen, K.; Shearer, J.; Catalano, V. J., Subtle Modulation of Cu4X4L2 Phosphine Cluster Cores Leads to Changes in Luminescence. *Inorg. Chem.* **2015,** 54, 6245-6256.
7. Chen, X. L.; Yu, R.; Wu, X. Y.; Liang, D.; Jia, J. H.; Lu, C. Z., A strongly greenish-blue-emitting Cu4Cl4 cluster with an efficient spin-orbit coupling (SOC): fast phosphorescence versus thermally activated delayed fluorescence. *Chem. Commun.* **2016,** 52, 6288-6291.
8. Musina, E. I.; Shamsieva, A. V.; Strelnik, I. D.; Gerasimova, T. P.; Krivolapov, D. B.; Kolesnikov, I. E.; Grachova, E. V.; Tunik, S. P.; Bannwarth, C.; Grimme, S.; Katsyuba, S. A.; Karasik, A. A.; Sinyashin, O. G., Synthesis of novel pyridyl containing phospholanes and their polynuclear luminescent copper(I) complexes. *Dalton Trans.* **2016,** 45, 2250-2260.
9. Huitorel, B.; El Moll, H.; Utrera-Melero, R.; Cordier, M.; Fargues, A.; Garcia, A.; Massuyeau, F.; Martineau-Corcos, C.; Fayon, F.; Rakhmatullin, A.; Kahlal, S.; Saillard, J. Y.; Gacoin, T.; Perruchas, S., Evaluation of Ligands Effect on the Photophysical Properties of Copper Iodide Clusters. *Inorg. Chem.* **2018,** 57, 4328-4339.
10. Yao, L.; Niu, G.; Li, J.; Gao, L.; Luo, X.; Xia, B.; Liu, Y.; Du, P.; Li, D.; Chen, C.; Zheng, Y.; Xiao, Z.; Tang, J., Circularly Polarized Luminescence from Chiral Tetranuclear Copper(I) Iodide Clusters. *J. Phys. Chem. Lett.* **2020,** 11, 1255-1260.
11. Olaru, M.; Rychagova, E.; Ketkov, S.; Shynkarenko, Y.; Yakunin, S.; Kovalenko, M. V.; Yablonskiy, A.; Andreev, B.; Kleemiss, F.; Beckmann, J.; Vogt, M., A Small Cationic Organo-Copper Cluster as Thermally Robust Highly Photo- and Electroluminescent Material. *J. Am. Chem. Soc.* **2020,** 142, 373-381.
12. Yam, V. W.-W.; Lee, W.-K.; Cheung, K.-K.; Crystall, B.; Phillips, D., Synthesis, structure, photophysics, time-resolved emission spectroscopy and electrochemistry of luminescent copper(I) acetylide complexes. *J. Chem. Soc., Dalton Trans.* **1996**, 3283-3287
13. Yam, V. W.-W.; Fung, W. K.-M.; Cheung, K.-K., Synthesis, Luminescence, and Electrochemistry of Mix-Capped Trinuclear Copper(I) Acetylide Complexes. X-ray Crystal Structures of [Cu3(μ-dppm)3(μ3-η1-C:CC6H4OMe-p)(μ3-η1-C:CC6H4OEt-p)]PF6and [Cu3(μ-dppm)3(μ3-η1-C:CC6H4OMe-p)(μ2-η1-C:CC6H4NO2-p)]PF6. *Organometallics* **1998,** 17, 3293-3298.
14. Dias, R. V. H.; Diyabalanage, K. V. H.; Eldabaja, G. M.; Elbjeirami, O.; Rawashdeh-Omary, A. M.; Omary, A. M., Brightly Phosphorescent Trinuclear Copper(I) Complexes of Pyrazolates: Substituent Effects on the Supramolecular Structure and Photophysics. *J. Am. Chem. Soc.* **2005,** 127, 7489-7501.
15. Artem'ev, A. V.; Doronina, E. P.; Rakhmanova, M. I.; Sutyrina, A. O.; Bagryanskaya, I. Y.; Tolstoy, P. M.; Gushchin, A. L.; Mazur, A. S.; Gusarova, N. K.; Trofimov, B. A., Luminescent CuI thiocyanate complexes based on tris(2-pyridyl)phosphine and its oxide: from mono-, di- and trinuclear species to coordination polymers. *New J. Chem.* **2016,** 40, 10028-10040.
16. Huang, M.-M.; Guo, Y.-M.; Shi, Y.; Zhao, L.; Niu, Y.-W.; Shi, Y.; Li, X.-L., Luminescent agostic Cu(I) complexes containing both trigonal planar and tetrahedral coordination modes. *Inorg. Chim. Acta* **2017,** 457, 107-115.
17. Xing, L. R.; Lu, Z.; Li, M.; Zheng, J.; Li, D., Revealing High-Lying Intersystem Crossing in Brightly Luminescent Cyclic Trinuclear Cu(I)/Ag(I) Complexes. *J. Phys. Chem. Lett.* **2020,** 11, 2067-2073.
18. Volz, D.; Baumann, T.; Flügge, H.; Mydlak, M.; Grab, T.; Bächle, M.; Barner-Kowollik, C.; Bräse, S., Auto-catalysed crosslinking for next-generation OLED-design. *J. Mater. Chem.* **2012,** 22, 20786-20790.
19. Zink, D. M.; Volz, D.; Baumann, T.; Mydlak, M.; Flügge, H.; Friedrichs, J.; Nieger, M.; Bräse, S., Heteroleptic, Dinuclear Copper(I) Complexes for Application in Organic Light-Emitting Diodes. *Chem. Mater.* **2013,** 25, 4471-4486.
20. Volz, D.; Zink, D. M.; Bocksrocker, T.; Friedrichs, J.; Nieger, M.; Baumann, T.; Lemmer, U.; Bräse, S., Molecular Construction Kit for Tuning Solubility, Stability and Luminescence Properties: Heteroleptic MePyrPHOS-Copper Iodide-Complexes and their Application in Organic Light-Emitting Diodes. *Chem. Mater.* **2013,** 25, 3414-3426.
21. Leitl, M. J.; Kuchle, F. R.; Mayer, H. A.; Wesemann, L.; Yersin, H., Brightly blue and green emitting Cu(I) dimers for singlet harvesting in OLEDs. *J. Phys. Chem. A* **2013,** 117, 11823-11836.
22. Nitsch, J.; Kleeberg, C.; Frohlich, R.; Steffen, A., Luminescent copper(I) halide and pseudohalide phenanthroline complexes revisited: simple structures, complicated excited state behavior. *Dalton Trans.* **2015,** 44, 6944-6960.
23. Nitsch, J.; Lacemon, F.; Lorbach, A.; Eichhorn, A.; Cisnetti, F.; Steffen, A., Cuprophilic interactions in highly luminescent dicopper(I)–NHC–picolyl complexes – fast phosphorescence or TADF? *Chem. Commun.* **2016,** 52, 2932-2935.
24. He, L. H.; Luo, Y. S.; Di, B. S.; Chen, J. L.; Ho, C. L.; Wen, H. R.; Liu, S. J.; Wang, J. Y.; Wong, W. Y., Luminescent Three- and Four-Coordinate Dinuclear Copper(I) Complexes Triply Bridged by Bis(diphenylphosphino)methane and Functionalized 3-(2'-Pyridyl)-1,2,4-triazole Ligands. *Inorg. Chem.* **2017,** 56, 10311-10324.
25. Schinabeck, A.; Leitl, M. J.; Yersin, H., Dinuclear Cu(I) Complex with Combined Bright TADF and Phosphorescence. Zero-Field Splitting and Spin-Lattice Relaxation Effects of the Triplet State. *J. Phys. Chem. Lett.* **2018,** 9, 2848-2856.
26. Zink, D. M.; Bachle, M.; Baumann, T.; Nieger, M.; Kuhn, M.; Wang, C.; Klopper, W.; Monkowius, U.; Hofbeck, T.; Yersin, H.; Bräse, S., Synthesis, structure, and characterization of dinuclear copper(I) halide complexes with P^N ligands featuring exciting photoluminescence properties. *Inorg. Chem.* **2013,** 52, 2292-2305.
27. Bizzarri, C.; Arndt, A. P.; Kohaut, S.; Fink, K.; Nieger, M., Mononuclear and dinuclear heteroleptic Cu(I) complexes based on pyridyl-triazole and DPEPhos with long-lived excited-state lifetimes. *J. Organomet. Chem.* **2018,** 871, 140-149.
28. Gracia, L. L.; Luci, L.; Bruschi, C.; Sambri, L.; Weis, P.; Fuhr, O.; Bizzarri, C., New Photosensitizers Based on Heteroleptic Cu(I) Complexes and CO2 Photocatalytic Reduction with [Ni(II)(cyclam)]Cl2. *Chem. Eur. J.* **2020,** 26, 9929 – 9937.
29. Bergmann, L.; Friedrichs, J.; Mydlak, M.; Baumann, T.; Nieger, M.; Bräse, S., Outstanding luminescence from neutral copper(I) complexes with pyridyl-tetrazolate and phosphine ligands. *Chem. Commun.* **2013,** 49, 6501-6503.
30. Leitl, M. J.; Krylova, V. A.; Djurovich, P. I.; Thompson, M. E.; Yersin, H., Phosphorescence versus thermally activated delayed fluorescence. Controlling singlet-triplet splitting in brightly emitting and sublimable Cu(I) compounds. *J. Am. Chem. Soc.* **2014,** 136, 16032-16038.
31. Linfoot, C. L.; Leitl, M. J.; Richardson, P.; Rausch, A. F.; Chepelin, O.; White, F. J.; Yersin, H.; Robertson, N., Thermally activated delayed fluorescence (TADF) and enhancing photoluminescence quantum yields of [Cu(I)(diimine)(diphosphine)](+) complexes-photophysical, structural, and computational studies. *Inorg. Chem.* **2014,** 53, 10854-10861.
32. Gneuß, T.; Leitl, M. J.; Finger, L. H.; Yersin, H.; Sundermeyer, J., A new class of deep-blue emitting Cu(I) compounds – effects of counter ions on the emission behavior. *Dalton Trans.* **2015,** 44, 20045-20055.
33. Czerwieniec, R.; Yersin, H., Diversity of copper(I) complexes showing thermally activated delayed fluorescence: basic photophysical analysis. *Inorg. Chem.* **2015,** 54, 4322-4327.
34. Schinabeck, A.; Rau, N.; Klein, M.; Sundermeyer, J.; Yersin, H., Deep blue emitting Cu(I) tripod complexes. Design of high quantum yield materials showing TADF-assisted phosphorescence. *Dalton Trans.* **2018,** 47, 17067-17076.
35. Brown, C. M.; Li, C.; Carta, V.; Li, W.; Xu, Z.; Stroppa, P. H. F.; Samuel, I. D. W.; Zysman-Colman, E.; Wolf, M. O., Influence of Sulfur Oxidation State and Substituents on Sulfur-Bridged Luminescent Copper(I) Complexes Showing Thermally Activated Delayed Fluorescence. *Inorg. Chem.* **2019,** 58, 7156-7168.
36. Liske, A.; Wallbaum, L.; Holzel, T.; Foller, J.; Gernert, M.; Hupp, B.; Ganter, C.; Marian, C. M.; Steffen, A., Cu-F Interactions between Cationic Linear N-Heterocyclic Carbene Copper(I) Pyridine Complexes and Their Counterions Greatly Enhance Blue Luminescence Efficiency. *Inorg. Chem.* **2019,** 58, 5433–5445.

37. Föller, J.; Ganter, C.; Steffen, A.; Marian, C. M., Computer-Aided Design of Luminescent Linear N-Heterocyclic Carbene Copper(I) Pyridine Complexes. *Inorg. Chem.* **2019,** 58, 5446–5456.
38. Volz, D.; Wallesch, M.; Grage, S. L.; Gottlicher, J.; Steininger, R.; Batchelor, D.; Vitova, T.; Ulrich, A. S.; Heske, C.; Weinhardt, L.; Baumann, T.; Bräse, S., Labile or stable: can homoleptic and heteroleptic PyrPHOS-copper complexes be processed from solution? *Inorg. Chem.* **2014,** 53, 7837-7847.
39. Wallesch, M.; Verma, A.; Flechon, C.; Flügge, H.; Zink, D. M.; Seifermann, S. M.; Navarro, J. M.; Vitova, T.; Gottlicher, J.; Steininger, R.; Weinhardt, L.; Zimmer, M.; Gerhards, M.; Heske, C.; Bräse, S.; Baumann, T.; Volz, D., Towards Printed Organic Light-Emitting Devices: A Solution-Stable, Highly Soluble Cu(I) - NHetPHOS. *Chem. Eur. J.* **2016,** 22, 16400-16405.
40. Czerwieniec, R.; Yu, J.; Yersin, H., Blue-light emission of Cu(I) complexes and singlet harvesting. *Inorg. Chem.* **2011,** 50, 8293-8301.
41. Hofbeck, T.; Monkowius, U.; Yersin, H., Highly efficient luminescence of Cu(I) compounds: thermally activated delayed fluorescence combined with short-lived phosphorescence. *J. Am. Chem. Soc.* **2015,** 137, 399-404.
42. Baranov, A. Y.; Berezin, A. S.; Samsonenko, D. G.; Mazur, A. S.; Tolstoy, P. M.; Plyusnin, V. F.; Kolesnikov, I. E.; Artem'ev, A. V., New Cu(I) halide complexes showing TADF combined with room temperature phosphorescence: the balance tuned by halogens. *Dalton Trans.* **2020,** 49, 3155-3163.
43. Tao, Y.; Yuan, K.; Chen, T.; Xu, P.; Li, H.; Chen, R.; Zheng, C.; Zhang, L.; Huang, W., Thermally activated delayed fluorescence materials towards the breakthrough of organoelectronics. *Adv. Mater.* **2014,** 26, 7931-7958.
44. Czerwieniec, R.; Leitl, M. J.; Homeier, H. H. H.; Yersin, H., Cu(I) complexes – Thermally activated delayed fluorescence. Photophysical approach and material design. *Coord. Chem. Rev.* **2016,** 325, 2-28.
45. Tang, C. W.; VanSlyke, S. A., Organic electroluminescent diodes. *Appl. Phys. Lett.* **1987,** 51, 913-915.
46. Bizzarri, C.; Spuling, E.; Knoll, D. M.; Volz, D.; Bräse, S., Sustainable metal complexes for organic light-emitting diodes (OLEDs). *Coord. Chem. Rev.* **2018,** 373, 49-82.
47. Bui, T. T.; Goubard, F.; Ibrahim-Ouali, M.; Gigmes, D.; Dumur, F., Recent advances on organic blue thermally activated delayed fluorescence (TADF) emitters for organic light-emitting diodes (OLEDs). *Beilstein J. Org. Chem.* **2018,** 14, 282-308.
48. Nakagawa, T.; Ku, S. Y.; Wong, K. T.; Adachi, C., Electroluminescence based on thermally activated delayed fluorescence generated by a spirobifluorene donor-acceptor structure. *Chem. Commun.* **2012,** 48, 9580-9582.
49. Rand, B. P.; Yersin, H.; Adachi, C.; Czerwieniec, R.; Hupfer, A.; van Elsbergen, V., Singlet harvesting with brightly emitting Cu(I) and metal-free organic compounds. **2012,** 8435, 843508-1-843508-10.
50. Bizzarri, C.; Hundemer, F.; Busch, J.; Bräse, S., Triplet emitters versus TADF emitters in OLEDs: A comparative study. *Polyhedron* **2018,** 140, 51-66.
51. Aslandukov, A. N.; Utochnikova, V. V.; Goriachiy, D. O.; Vashchenko, A. A.; Tsymbarenko, D. M.; Hoffmann, M.; Pietraszkiewicz, M.; Kuzmina, N. P., The development of a new approach toward lanthanide-based OLED fabrication: new host materials for Tb-based emitters. *Dalton Trans.* **2018,** 47, 16350-16357.
52. Utochnikova, V. V.; Latipov, E. V.; Dalinger, A. I.; Nelyubina, Y. V.; Vashchenko, A. A.; Hoffmann, M.; Kalyakina, A. S.; Vatsadze, S. Z.; Schepers, U.; Bräse, S.; Kuzmina, N. P., Lanthanide pyrazolecarboxylates for OLEDs and bioimaging. *J. Lumin.* **2018,** 202, 38-46.
53. Kalyakina, A. S.; Utochnikova, V. V.; Sokolova, E. Y.; Vashchenko, A. A.; Lepnev, L. S.; Van Deun, R.; Trigub, A. L.; Zubavichus, Y. V.; Hoffmann, M.; Mühl, S.; Kuzmina, N. P., OLED thin film fabrication from poorly soluble terbium o-phenoxybenzoate through soluble mixed-ligand complexes. *Org. Electron.* **2016,** 28, 319-329.
54. Koshelev, S. D.; Chikineva, Y. T.; Kozhevnikova (Khudoleeva), Y. V.; Medvedko, V. A.; Vashchenko, A. A.; Goloveshkin, S. A.; Tsymbarenko, M. D.; Averin, A. A.; Meschkov, A.; Schepers, U.; Vatsadze, Z. S.; Utochnikova, V. V., On the design of new europium heteroaromatic carboxylates for OLED application. *Dyes Pigments* **2019,** 170, 107604.
55. Utochnikova, V. V.; Solodukhin, N. N.; Aslandukov, A. N.; Marciniak, L.; Bushmarinov, I. S.; Vashchenko, A. A.; Kuzmina, N. P., Lanthanide tetrafluorobenzoates as emitters for OLEDs: New approach for host selection. *Org. Electron.* **2017,** 44, 85-93.
56. Xu, Z.; Tang, B. Z.; Wang, Y.; Ma, D., Recent advances in high performance blue organic light-emitting diodes based on fluorescence emitters. *J. Mater. Chem. C* **2020,** 8, 2614-2642.
57. Zhao, J.-H.; Hu, Y.-X.; Lu, H.-Y.; Lü, Y.-L.; Li, X., Progress on benzimidazole-based iridium(III) complexes for application in phosphorescent OLEDs. *Org. Electron.* **2017,** 41, 56-72.
58. Hu, Y.-X.; Wen-Ze He, X. X.; Tang, Z.-J.; Lv, Y.-L.; Li, X.; Zhang, D.-Y., Recent developments in benzothiazole-based iridium(Ⅲ) complexes for application in OLEDs as electrophosphorescent emitters. *Org. Electron.* **2019,** 66, 126-135.
59. Wang, X.; Wang, S., Phosphorescent Pt(II) Emitters for OLEDs: From Triarylboron-Functionalized Bidentate Complexes to Compounds with Macrocyclic Chelating Ligands. *Chem. Rec.* **2019,** 19, 1693-1709.
60. Wang, J.; Liang, J.; Xu, Y.; Liang, B.; Wei, J.; Li, C.; Mu, X.; Ye, K.; Wang, Y., Purely Organic Phosphorescence Emitter-Based Efficient Electroluminescence Devices. *J. Phys. Chem. Lett.* **2019,** 10, 5983-5988.
61. Minaev, B.; Baryshnikov, G.; Agren, H., Principles of phosphorescent organic light emitting devices. *Phys. Chem. Chem. Phys.* **2014,** 16, 1719-1758.
62. Lee, J.-H.; Chen, C.-H.; Lee, P.-H.; Lin, H.-Y.; Leung, M.-k.; Chiu, T.-L.; Lin, C.-F., Blue organic light-emitting diodes: current status, challenges, and future outlook. *J. Mater. Chem. C* **2019,** 7, 5874-5888.
63. Zhang, Q.; Komino, T.; Huang, S.; Matsunami, S.; Goushi, K.; Adachi, C., Triplet Exciton Confinement in Green Organic Light-Emitting Diodes Containing Luminescent Charge-Transfer Cu(I) Complexes. *Adv. Funct. Mater.* **2012,** 22, 2327-2336.
64. Huang, T.; Jiang, W.; Duan, L., Recent progress in solution processable TADF materials for organic light-emitting diodes. *J. Mater. Chem. C* **2018,** 6, 5577-5596.
65. Rizzo, F.; Cucinotta, F., Recent Developments in AIEgens for Non-doped and TADF OLEDs. *Isr. J. Chem.* **2018,** 58, 874-888.
66. Busch, J. M.; Zink, D. M.; Di Martino-Fumo, P.; Rehak, F. R.; Boden, P.; Steiger, S.; Fuhr, O.; Nieger, M.; Klopper, W.; Gerhards, M.; Bräse, S., Highly soluble fluorine containing Cu(I) AlkylPyrPhos TADF complexes. *Dalton Trans.* **2019,** 48, 15687-15698.
67. Churchill, R. M.; DeBoer, G. B.; Donovan, J. D., Molecules with an M4X4 core. IV.1-3 Crystallographic Detection of a “Step” Configuration for the CuI4I4 Core in Tetrameric Triphenylphosphinecopper(I) Iodide, [PPh3CuI]4. *Inorg. Chem.* **1975,** 14, 617-623.
68. Volz, D.; Nieger, M.; Friedrichs, J.; Baumann, T.; Bräse, S., How the quantum efficiency of a highly emissive binuclear copper complex is enhanced by changing the processing solvent. *Langmuir* **2013,** 29, 3034-3044.
69. Zink, D. M.; Baumann, T.; Friedrichs, J.; Nieger, M.; Bräse, S., Copper(I) complexes based on five-membered P^N heterocycles: structural diversity linked to exciting luminescence properties. *Inorg. Chem.* **2013,** 52, 13509-13520.
70. Volz, D.; Hirschbiel, A. F.; Zink, D. M.; Friedrichs, J.; Nieger, M.; Baumann, T.; Bräse, S.; Barner-Kowollik, C., Highly efficient photoluminescent Cu(I)–PyrPHOS-metallopolymers. *J. Mater. Chem. C* **2014,** 2, 1457-1462.
71. Mohankumar, M.; Holler, M.; Meichsner, E.; Nierengarten, J. F.; Niess, F.; Sauvage, J. P.; Delavaux-Nicot, B.; Leoni, E.; Monti, F.; Malicka, J. M.; Cocchi, M.; Bandini, E.; Armaroli, N., Heteroleptic Copper(I) Pseudorotaxanes Incorporating Macrocyclic Phenanthroline Ligands of Different Sizes. *J. Am. Chem. Soc.* **2018,** 140, 2336-2347.
72. Shi, S.; Jung, M. C.; Coburn, C.; Tadle, A.; Sylvinson, M. R. D.; Djurovich, P. I.; Forrest, S. R.; Thompson, M. E., Highly Efficient Photo- and Electroluminescence from Two-Coordinate Cu(I) Complexes Featuring Nonconventional N-Heterocyclic Carbenes. *J. Am. Chem. Soc.* **2019,** 141, 3576-3588.
73. Armaroli, N.; Accorsi, G.; Holler, M.; Moudam, O.; Nierengarten, J. F.; Zhou, Z.; Wegh, R. T.; Welter, R., Highly

Luminescent CuI Complexes for Light-Emitting Electrochemical Cells. *Advanced Materials* **2006,** 18, (10), 1313-1316.
74. Felder, D.; Nierengarten, J.-F.; Barigelletti, F.; Ventura, B.; Armaroli, N., Highly Luminescent Cu(I)−Phenanthroline Complexes in Rigid Matrix and Temperature Dependence of the Photophysical Properties. *J. Am. Chem. Soc.* **2001,** 123, 6291 - 6299.
75. Kobayashi, T.; Niwa, A.; Takaki, K.; Haseyama, S.; Nagase, T.; Goushi, K.; Adachi, C.; Naito, H., Contributions of a Higher Triplet Excited State to the Emission Properties of a Thermally Activated Delayed-Fluorescence Emitter. *Physical Review Applied* **2017,** 7, (0340021-03400210).
76. de Silva, P., Inverted Singlet-Triplet Gaps and Their Relevance to Thermally Activated Delayed Fluorescence. *J. Phys. Chem. Lett.* **2019,** 10, 5674-5679.
77. Eizner, E.; Martínez-Martínez, L. A.; Yuen-Zhou, J.; Kéna-Cohen, S., Inverting singlet and triplet excited states using strong light-matter coupling. *Sci. Adv.* **2019,** 5, 2-8.
78. Zhang, X.; Guo, X.; Chen, Y.; Wang, J.; Lei, Z.; Lai, W.; Fan, Q.; Huang, W., Highly efficient red phosphorescent organic light-emitting devices based on solution-processed small molecular mixed-host. *J. Lumin.* **2015,** 161, 300-305.
79. Matsusue, N.; Ikame, S.; Suzuki, Y.; Naito, H., Charge carrier transport in an emissive layer of green electrophosphorescent devices. *Appl. Phys. Lett.* **2004,** 85, 4046-4048.
80. Kang, J.-W.; Lee, S.-H.; Park, H.-D.; Jeong, W.-I.; Yoo, K.-M.; Park, Y.-S.; Kim, J.-J., Low roll-off of efficiency at high current density in phosphorescent organic light emitting diodes. *Appl. Phys. Lett.* **2007,** 90, 223508.
81. Namdas, E. B.; Anthopoulos, T. D.; Samuel, I. D. W.; Frampton, M. J.; Lo, S.-C.; Burn, P. L., Simple color tuning of phosphorescent dendrimer light emitting diodes. *Appl. Phys. Lett.* **2005,** 86, 161104.
82. Jou, J.-H.; Sun, M.-C.; Chou, H.-H.; Li, C.-H., Efficient pure-white organic light-emitting diodes with a solution-processed, binary-host employing single emission layer. *Appl. Phys. Lett.* **2006,** 88, 141101.
83. Kim, T.-Y.; Jung, J.-H.; Kim, J.-B.; Moon, D.-G., Achieving high efficiency by high temperature annealing of hole transporting polymer layer in solution-processed organic light-emitting devices. *Synth. Met.* **2017,** 232, 167-170.
84. Thejo Kalyani, N.; Dhoble, S. J., Organic light emitting diodes: Energy saving lighting technology—A review. *Renew. Sust. Energ. Rev.* **2012,** 16, 2696-2723.
85. Zhang, L.; Li, B.; Yue, S.; Li, M.; Hong, Z.; Li, W., A terbium (III) complex with triphenylamine-functionalized ligand for organic electroluminescent device. *J. Lumin.* **2008,** 128, 620-624.
86. Fan, C.; Chen, Y.; Liu, Z.; Jiang, Z.; Zhong, C.; Ma, D.; Qin, J.; Yang, C., Tetraphenylsilane derivatives spiro-annulated by triphenylamine/carbazole with enhanced HOMO energy levels and glass transition temperatures without lowering triplet energy: host materials for efficient blue phosphorescent OLEDs. *J. Mater. Chem. C* **2013,** 1, 463-469.
87. Liu, T.; Foo, Y.; Zapien, J. A.; Li, M.; Tsang, S. W., A generalized Stark effect electromodulation model for extracting excitonic properties in organic semiconductors. *Nat. Commun.* **2019,** 10, 1-11.
88. Miśnik, M.; Falkowski, K.; Mróz, W.; Stampor, W., Electromodulation of photoluminescence in vacuum-evaporated films of bathocuproine. *Chem. Phys.* **2013,** 410, 45-54.
89. Yang, X.; Hernandez-Martinez, P. L.; Dang, C.; Mutlugun, E.; Zhang, K.; Demir, H. V.; Sun, X. W., Electroluminescence Efficiency Enhancement in Quantum Dot Light-Emitting Diodes by Embedding a Silver Nanoisland Layer. *Adv. Opt. Mater.* **2015,** 3, 1439-1445.
90. Yang, H.; Holloway, P. H., Electroluminescence from Hybrid Conjugated Polymer - CdS:Mn/ZnS Core/Shell Nanocrystals Devices. *J. Phys. Chem. B* **2003,** 107, 9705-9710.
91. Chaieb, A.; Vignau, L.; Brown, R.; Wantz, G.; Huby, N.; François, J.; Dagron-Lartigau, C., PL and EL properties of oligo(p-phenylene vinylene) (OPPV) derivatives and their applications in organic light-emitting diodes (OLED). *Opt. Mater.* **2008,** 31, 68-74.

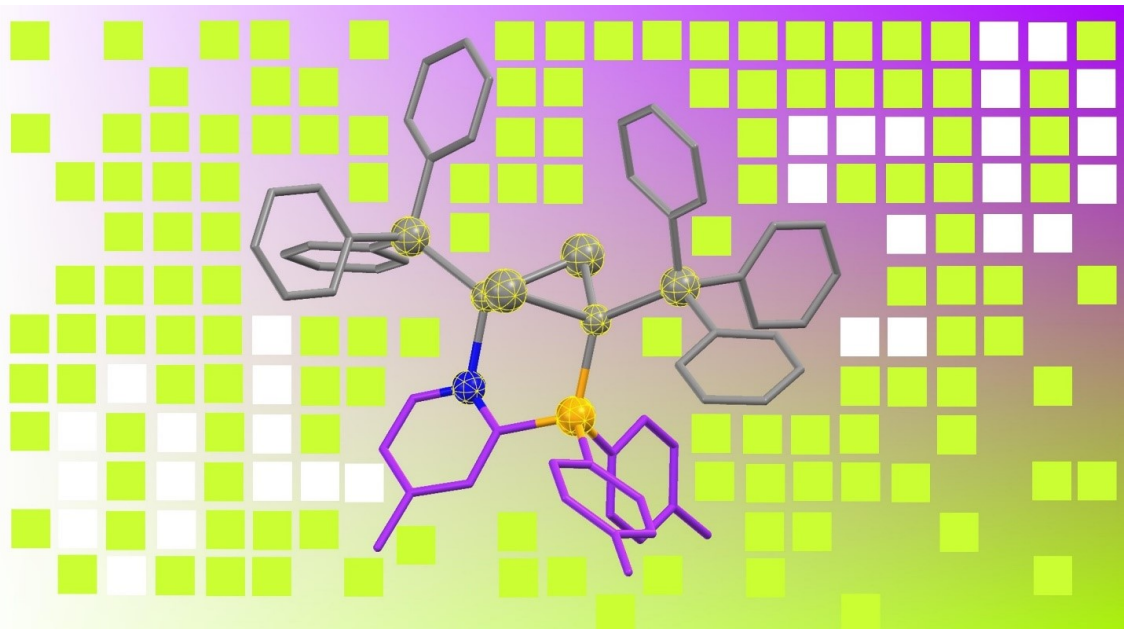

Luminescent dinuclear Cu(I) complexes bridged by novel phosphinopyridine-ligands with various substituents on the phosphine moiety were synthesized as OLED-emitters and were confirmed by molecular structures. Photophysical studies of the complexes (89% PLQY in powder) were supported by theoretical computations. Various solution-processed OLEDs with different heterostructures were built of the Cu-emitters, reaching a high brightness of 5900 Cd/m² and a good current efficiency of 3.79 Cd/A with an OLED stack architecture of ITO/PEDOT-PSS/poly-TPD/Cu(I) emitter:CBP:TcTA(7:3)/TPBi/LiF/Al.